Journal of Volcanology and Geothermal Research 432 (2022) 107674

Contents lists available at ScienceDirect

Journal of Volcanology and Geothermal Research

journal homepage: www.journals.elsevier.com/journal-of-volcanology-and-geothermal-research

The effects of unsteady effusion rates on lava flow emplacement: Insights from laboratory analogue experiments

S.I. Peters [a,c,*], A.B. Clarke [a,b], E.L. Rader [c]

[a] School of Earth and Space Exploration, Arizona State University, Tempe, AZ 85281, USA
[b] Istituto Nazionale di Geofisica e Vulcanologia, Sezione di Pisa, Pisa, Italy
[c] Department of Geography and Geological Sciences, University of Idaho, Moscow, ID 83843, USA

ARTICLE INFO

Keywords:
Volcano
Lava flow
Crust
Experiment
Laboratory

ABSTRACT

The phenomenology of lava flow emplacement involves complex physical processes related to crystallization, eruption rate, temperature, crust solidification, and a variety of other factors. Changes in effusion rate are a natural part of lava flow emplacement and can complicate lava flow morphology and propagation. Analog experiments are a useful tool for investigating the role of changing effusion rates on flow propagation because they allow reasonably precise control of conditions and detailed documentation of resulting flows. Experimental datasets that investigate the impact of variable effusion rates on flow propagation can be used to enhance fundamental understanding of flow processes and to inform numerical models for hazards forecasts. In this study, we address the effects of decreasing and increasing eruption rates (Q) on four emplacement modes common to lava flows: *resurfacing, marginal breakouts, inflation, and lava tubes*. Laboratory analogue experiments using polyethylene glycol (PEG) 600 wax were used to derive Ψ, a dimensionless parameter that relates crust formation (t_s) and lateral advection (t_a) timescales of a viscous gravity current. We conducted 120 experiments using a peristaltic pump to inject dyed PEG wax into a chilled bath (~ 0 °C) in a tank with a roughened base at a slope of 0°. The experiments were divided into two conditions: decreasing Q with time (condition 1) and increasing Q with time (condition 2). We controlled for volume of extruded wax, temperature, instantaneous eruption rate, Ψ, and duration of the decrease or increase in eruption rate. Results indicate that the duration of the pulsatory eruption rate, the experimental condition, initial Ψ, and the extruded volume influence the presence and strength of a crust (or lack thereof) which in turn influences the onset and extent of the four emplacement modes investigated. Prolonged increase in eruption rates favored resurfacing, widespread marginal breakouts and flow advancement, inflation, and some tube formation, while the specific morphology and area covered was controlled by an extensive, coherent crust, which in turn depended on initial Ψ and duration of the initial eruptive stage. Prolonged decreasing eruption rates promoted localized marginal breakouts, inflation, and tube formation. The duration of the pulse during the eruption rate change affected the likelihood and/or significance of the mode of emplacement. Similar observations were made on the early stages of the 2021 Fagradalsfjall eruption in Iceland to demonstrate the utility of the wax experiments in interpreting natural systems.

Plain language summary: Predicting where lava will flow remains challenging due to the complex variables affecting its propagation. Lava is a multiphase fluid made of solids, liquids, and gas. In addition, as it cools, it forms a crust that can affect the flow. The eruption of lava is rarely steady over short and long timescales. This variability in eruption rate can also affect lava flow propagation and hence affect its predictability. Such variability in eruption rate may cause the flow to grow in thickness, in length, in width, or all of these simultaneously, and the style of growth affects the area impacted and controls where the flow is most hazardous. While numerical models have been useful in simulating flow advance on slopes, these models often simplify lava flow geometry and propagation mechanics. Laboratory analogue experiments allow for the reproduction of complex physics and morphology that closer approximate processes observed in nature. In this study, 120 experiments using PEG 600 – a water-soluble wax – were used to simulate lava flow emplacement under unsteady vent conditions. Flows were emplaced while increasing or decreasing the eruption rate during an eruption and the duration of the increase or decrease in eruption rate was varied along with other flow conditions. In the experiments, increasing or decreasing eruption rate at the vent, along with other parameters, impacted the

* Corresponding author at: Department of Earth and Spatial Sciences, University of Idaho, Moscow, ID 83844, USA.
E-mail address: seanpeters@uidaho.edu (S.I. Peters).

https://doi.org/10.1016/j.jvolgeores.2022.107674
Received 23 March 2022; Received in revised form 13 September 2022; Accepted 19 September 2022
Available online 28 September 2022

formation of a cohesive or brittle crust, which in turn exerted strong control on whether the flows thickened or lengthened, affecting the area impacted and flow morphology. We map out lava flow characteristics in terms of these vent conditions, and compare our findings to a real eruption in Iceland.

1. Introduction

1.1. Lava flow emplacement and morphology

Lava flows are one of the most common landforms on the Earth and one of the primary hazards of volcanic eruptions [e.g., Crisp, 1984; Pinkerton, 1987; Francis and Oppenheimer, 2003]. The emplacement, propagation, and morphology of lava flows is dictated by a variety of factors, including mean overall effusion rate, changes in effusion rate, cooling, crystallization, solidification; degassing, topography, and erupted volume [e.g., Walker, 1973; Hulme, 1974; Malin, 1980; Pinkerton, 1987; Fink and Griffiths, 1990, Fink and Griffiths, 1992; Dragoni and Tallarico, 1994; Gregg and Fink, 2000; Griffiths, 2000; Belousov et al., 2015]. Despite their abundance, the phenomenology of lava flow emplacement remains poorly constrained due to its inherent complexity [Pinkerton, 1987; Fink and Griffiths, 1990, Fink and Griffiths, 1992; Gregg and Fink, 2000; Rader et al., 2017]. Real-time or near real-time observations, although hindered by some limitations, have aided our fundamental understanding of lava flow emplacement [e.g., Walker, 1973; Wadge, 1981; Pinkerton, 1987; Belousov et al., 2015].

In addition, better understanding of lava flow emplacement processes is invaluable in reconstructing the formation and evolutionary history of planetary surfaces. Lava flows are common, covering ~65% of the Earth's surface, ~80% of Venus, ~50% of Mars, and ~ 20% of the Moon, with more exotic compositions observed on Outer Solar System satellites [e.g., Greeley and Spudis, 1981; Fink et al., 1983; Crisp, 1984; Francis and Oppenheimer, 2003; Ivanov and Head, 2013; Peters et al., 2021]. Therefore, the behavior – i.e., dynamics and emplacement – of these lava flows is crucial to learning about the formation and evolution of the surface of Earth and other planetary bodies [e.g., Gregg and Fink, 1996; Peters et al., 2021].

Our understanding of lava flows, primarily basaltic in composition, comes largely from historical and contemporary eruptions – some of which have been witnessed, recorded, and subsequently analyzed – in Hawai'i, Iceland, Sicily, and on the seafloor [e.g., Walker, 1973; Greeley, 1972, 1987; Malin, 1980; Pinkerton, 1987; Wadge, 1981; Gregg and Smith, 2003]. Additionally, localities such as the Deccan Traps and Columbia River Basalts provide upper endmember examples of the scale of lava flow constructs, given sufficient time and volume of material [e.g., Danes, 1972; Self et al., 1996; Sheth, 2006; Rader et al., 2017].

The morphology of a lava flow is determined by its complex and changing rheology, effusion rate, and preexisting topography [e.g., Pinkerton, 1987; Fink and Griffiths, 1990, Fink and Griffiths, 1992; Dragoni and Tallarico, *1994*; Gregg and Fink, 2000; Griffiths, 2000; Cashman et al., 2006]. Walker [1973] argued that the length of a lava flow is determined primarily by the eruption rate, whereas Malin [1980] tied lava flow length to the total volume of erupted material. Fink and Griffiths [1990] and Cashman et al. [2006] highlighted that the readiness to form a crust controls the morphology of lava flows, while Gregg and Fink [2000] observed that flows erupted on steeper slopes are narrower and longer. Lava flows have a variety of morphologies which correspond to a range of emplacement modes and propagation rates, from channelized flows to pāhoehoe sheet flows to pillow lavas [e.g., Hulme, 1974; Hon et al., 1994; Gregg and Keszthelyi, 2004]. The morphology of lava flows is closely connected to and influenced by the mode of emplacement.

1.2. Modes of emplacement

In this study, we focus on four modes of emplacement which control how lava is transported and distributed in a flow, and ultimately control propagation rate and final area covered by a flow. These modes are: resurfacing, marginal breakouts, inflation, and tube formation. Resurfacing is defined here as the process by which lava covers a preexisting flow surface during the same eruptive event (Fig. 1c). We opted for a generalized definition of this process in order to capture the many manifestations resurfacing can take depending on flow conditions in natural lava flows. Resurfacing is essentially a breakout or overflow onto the surface of a lava flow, which leads to stacking of lobes or the repaving of the flow surface. Resurfacing is a component of compound lava flows, which consist of overlapping flow lobes [e.g., Walker, *1973*; Blake and Bruno, 2000].

Marginal breakouts, on the other hand, involve transport of lava under the flow crust, followed by rupturing of the crust at the flow margin and subsequent flow propagation and an increase in flow area (Fig. 1b). Breakouts occur due to overpressurization of the liquid core due to continuous lava influx causing the viscoelastic crust to rupture at the distal edges of the flow [e.g., Hon et al., 1994; Hoblitt et al., 2012; Tuffen et al., 2013; Rader et al., 2017]. Sudden increases in flow rate also have the same effect of increasing pressure and promoting breakouts [e.g., Hoblitt et al., 2012].

Inflation is the endogenic growth of a lava flow via the emplacement of molten lava in its core beneath the crust, which results in the thickening of the flow [Fig. 1d; e.g., Hon et al., 1994; Hoblitt et al., 2012]. Inflation has been observed to thicken lava flows from centimeters to tens of meters, and is thought to occur in many lava flows observed in the Deccan Traps and the Columbia River Basalts [e.g., Self et al., 1996; Sheth, 2006; Tuffen et al., 2013; Rader et al., 2017] as well as in rhyolitic and highly viscous andesitic lava flows [e.g., Tuffen et al., 2013; Carr et al., 2019].

Lava tubes are a common construct in lava flow fields and can form in a number of ways including the roofing over of open channels and the consolidation of interconnected pathways within pāhoehoe flows. Lava tubes are discrete pathways in a flow and the overlying crust insulates liquid lava allowing it to retain its heat and travel farther (Fig. 1a). As such, lava tubes tend to form during longer-lived eruptions and expand lava flow fields [e.g., Greeley, 1972, 1987; Belousov et al., 2015]. While lava tubes can occur in inflated pāhoehoe sheet flow fields, lava tubes are localized and also occur independently of inflation [e.g., Greeley, 1972; Greeley, 1987]. Knowing under what conditions these emplacement modes operate is fundamental to aiding in hazards mitigation and establishing a framework for volcanic conditions on other planets, such as Mars [e.g., Greeley, 1972, 1987; Pinkerton, 1987; Gregg and Fink, 1996].

1.3. Eruption tempo

The eruption of lava flows is a dynamic process with a host of variables that evolve as the eruption progresses and the lava flow propagates away from the vent. While the average effusion rate is typically calculated and cited in the literature for a given volcanic eruption, the effusion rate at volcanic vents often varies with time and may do so rapidly over short timescales [e.g., Walker, 1973; Wadge, 1981; Tarquini and d'Michieli Vitturi, 2014; Dietterich et al., 2017; Rader et al., 2017]. Basaltic eruptions typically experience a large increase in effusion rate shortly after the eruption commences followed by exponential decline after some maximum value is achieved, although periodic spikes in the eruption rate can occur [Wadge, 1981; Belousov et al., 2015]. As such, the average effusion rate can underestimate the eruptive conditions at the vent early in an eruption and overestimate the conditions later in an

eruption. Furthermore, local flow rates fluctuate all across a flow field due to local changes in slope, solidification conditions, among other factors. Therefore, understanding how flow rates impact emplacement mechanisms is also relevant to distal but active portions of a flow field.

Effusion rates can fluctuate due to the injection of more magma into subsurface storage, widening of the conduit, thermal contraction of the magma, among other mechanisms [e.g., Wadge, 1981; Bailey et al., 2006; Bonny and Wright, 2017; Patrick et al., 2019]. These fluctuations can be small – due to blockages within a specific region of the flow itself – or large – due to activity at the volcanic vent. For example, during channelized flows on Mt. Etna cyclical fluxes in volumetric flow rates at the vent have been observed to generally involve dramatic increases in flow rates followed by a more gradual decrease of the flow rate [Bailey et al., 2006]. Rapid increases in effusion rate are termed *pulse* events and they can have a huge impact on flow emplacement, promoting overspills, flow blockages, breakouts, the remobilization of stationary flows, and the development of new channels [e.g., Peterson and Tilling, 1980; Baloga and Pieri, 1986; Hon et al., 1994; Bailey et al., 2006]. While Wadge [1981] characterizes most effusive eruptions by a sharp increase in effusion rate followed by an exponential decline until the eruption ceases, Bonny and Wright [2017] observed different effusion rate patterns characterized by exponential decline in effusion rate, double pulse (i.e., double increases in effusion rate), or repeated increases and decreases in effusion rate that lack a consistent pattern. Changes in effusion rate at the vent can impact the flow rate at the lava flow front, the morphology of the flow, and influence which emplacement modes are likely to occur [Wadge, 1981; Bailey et al., 2006; Patrick et al., 2019]. Previous studies suggest that, under steady flow rates, inflation tends to

Fig. 1. Field examples of the four modes of emplacement common to lava flows that are observed in this study. (a) Chilled crust of a small tube at Holuhraun, Iceland (b) Example of a marginal breakout at the edge of a pāhoehoe flow in Hawai'i. (c) Resurfacing shown at Fagradalsfjall, Iceland. (d) Inflation thickens lava flows from within a molten core, illustrated by dashed arrows showing a lobe the grew vertically. Image from the Blue Dragon Flow in southern Idaho, dashed arrows are approximately 10 cm. (For interpretation of the references to color in this figure legend, the reader is referred to the web version of this article.)

occur under low eruption rates, while lava tubes – depending on their formation mechanism – form at low to moderate eruption rates [e.g., Greeley, 1987; Hon et al., 1994]. However, this existing framework does not consider short-term fluctuations in flow rate.

Variability in lava flow dynamics remains a challenge to hazards assessment. For example, increasing effusion rates have been observed to remobilize nearly stationary 'a'ā flows [Peterson and Tilling, 1980]. In the 1973 lava flow in Heimaey, Iceland, a water-cooled lava flow stopped propagating until the accumulation of material behind the flow front caused a breakout that destroyed 100 homes [Pinkerton, 1987]. A similar instance of a lava flow deviating from its expected flow path occurred during the 2012–2013 effusive eruption sequence of Tolbachik volcano in Kamchatka, Russia; as the eruption rate at the vent decreased, the flow front ceased and the flow increased in width and thickness (inflation) [Belousov et al., 2015]. Tuffen et al. [2013] demonstrated that lava flows, in their case rhyolitic, can continue to advance and pose a hazard even after effusion at the vent has ceased.

1.4. Lava flow modelling

In order to prevent human and economic losses, numerical modelling is used extensively to simulate lava flow propagation and inundation and to predict the path of future lava flows [e.g., Pinkerton, 1987; Harris and Rowland, 2001; Felpeto et al., 2001; Favalli et al., 2005; Connor et al., 2012; Dietterich et al., 2017; D'Michieli Vitturi and Tarquini, 2018]. Inundation models are commonly used to simulate flow emplacement in order to evaluate hazards without the requirement of numerical parameters for lava flow properties, which may be unknown or difficult to estimate [e.g., Felpeto et al., 2001; Favalli et al., 2005; Dietterich et al., 2017; D'Michieli Vitturi and Tarquini, *2018*]. However, inundation models do not capture the complete physics of lava flow emplacement, but instead rely on simplified propagation rules and probabilistic assessments [e.g., Felpeto et al., 2001; Favalli et al., 2005; Dietterich et al., 2017; D'Michieli Vitturi and Tarquini, *2018*]. Propagation-focused models, such as FLOWGO and MAGFLOW, are very effective at simulating open channel flow propagation and flow on steep or confined slopes, but they cannot predict emplacement mode or changes in emplacement mode a priori and they do not capture the dynamics of emplacement styles such as breakouts, inflation, and tube formation [Harris and Rowland, 2001; Rowland et al., 2004; Ganci et al., 2012; Del Negro et al., 2013]. The predictive capability of models is often validated by demonstrating how well a model replicates well-documented flows [e.g., Connor et al., 2012; Dietterich et al., 2017; D'Michieli Vitturi and Tarquini, *2018*; DeGraffenried et al., *2021*]. Understanding what influences the propagation rate and emplacement mode of lava flows is key to unraveling their complex dynamics, which in turn can be used to improve existing models, their predictive capabilities, and their utility in hazards mitigation.

Physics-based models, such as FLOWGO, MAGFLOW, LavaSIM, and a 3-D lava flow model developed in OpenFOAM by Dietterich et al. [2017], to name a few, account for temporal variations and thermo-rheological aspects of lava flows, but these can be computationally expensive and difficult to employ in real-time hazard assessment [Harris and Rowland, 2001; Rowland et al., 2004; Ganci et al., 2012; Del Negro et al., 2013; Dietterich et al., 2017]. FLOWGO models lava propagation by solving a steady-state force balance between a downslope driving force and viscous retarding forces in a Bingham fluid, which depend on rheological properties of the lava flow and flow geometry. While it accounts for a surface crust, the primary disadvantage of FLOWGO is its exclusive applicability to lava flows confined to a channel [Harris and Rowland, 2001; Rowland et al., 2004]. MAGFLOW allows interaction with complex topography and consequent complex flow geometry, but it assumes a steady flux from the vent and does not account for crust formation nor for inflation beneath a crust. MAGFLOW is typically used in hazards predictions by taking a Monte Carlo approach [Ganci et al., 2012; Del Negro et al., 2013; Capello et al., 2015]. LavaSIM, a 3-D convective analysis model that treats lava as a two-phase liquid (i.e., crust and liquid lava) allows for the evaluation of overprinting of solidified lava flows by subsequent lava flows, levee formation, and lava tube formation [Hidaka et al., *2005*]. The 3-D model developed in OpenFOAM can simulate changes in viscosity and rheology (i.e., crust formation) as well [Jasak et al., 2007; Dietterich et al., 2017]. Like many models, when reproducing historical lava flows, LavaSIM and OpenFOAM depend on inputs that accurately capture processes at the time of lava flow emplacement.

These models illustrate the key difficulties related to emplacement modes – physics-based models currently must assume from the onset a simplified emplacement mode that ignores or approximates the role of the lava crust. Many lava flows pass through two or more crust-influenced modes during their lifetimes – resurfacing, inflation followed by toe breakout, tube formation, and channelization testifying to the complexity of numerically simulating the emplacement of real lava flows. Laboratory analogue experiments, on the other hand, elucidate controls on mode of emplacement and therefore have the potential to better constrain models [e.g., Dietterich et al., 2017]. While laboratory experiments also rely on simplifications and cannot recreate every aspect of a lava flow, they offer the opportunity to investigate the complex phenomenology of lava flows [Hallsworth et al., 1987; Fink and Griffiths, 1990, Fink and Griffiths, 1992; Griffiths and Fink, 1992, 1993; Griffiths and Fink, 1997; Blake and Bruno, 2000; Gregg and Fink, 2000; Griffiths, 2000] and relate mode of emplacement to lava characteristics and eruption rate.

1.5. Laboratory analogue experiments

Previous studies [e.g., Hallsworth et al., 1987; Fink and Griffiths, 1990; Griffiths and Fink, 1992, 1993; Gregg and Fink, 1996, 2000; Griffiths and Fink, 1997; Blake and Bruno, 2000; Soule and Cashman, 2004; Kerr et al., 2006; Rader et al., 2017, *and those contained in* Lev et al., 2019] have established the utility of laboratory analogue experimentation, in particular, the use of polyethylene glycol wax (PEG) – a commercial grade polymer used in the production of food and pharmaceutical products – in simulating lava flows due to its readiness to form a crust and temperature dependent viscosity [Soule and Cashman, 2004]. Fink and Griffiths [1990] used PEG experiments to derive a dimensionless parameter, Ψ. Ψ describes the ability of a viscous gravity current to transfer heat either via the surface of the fluid or through lateral advection [Fink and Griffiths, 1990, Fink and Griffiths, 1992; Griffiths and Fink, 1997; Gregg and Fink, 2000]. Accordingly, Ψ is defined as the ratio of the timescale of surface crust formation (t_s) to the timescale of flow advancement (t_a).

$$\Psi = \frac{t_s}{t_a} \tag{1}$$

Alternatively, the formula can be written with respect to the modified Peclet number (Π), crustal cooling time (τ_s), and temperature differences among the ambient fluid, the erupted liquid, and the solidification temperature of the liquid (θ_s). We calculate modified Π according to the following expression:

$$\Pi = \left(\frac{g'}{\nu}\right)^{\frac{2}{3}} \kappa^{\frac{1}{3}} \lambda Pe^{\frac{1}{3}} \tag{2}$$

The modified Peclet number (Π) incorporates the traditional Peclet number (thermal advection rate/thermal diffusion rate), thermal diffusivity, and a dimensionless timescale that quantifies the time it takes the contact temperature to decrease to that of the ambient environment (i.e., the water bath in the case of Fink and Griffiths, 1990 and this study, see Methodology section). Modified Π also includes the effects of reduced gravity (g'), kinematic viscosity (ν), thermal diffusivity of the wax or lava (κ), and the timescale (λ) over which the contact temperature of the wax or lava reaches the temperature of the ambient environment far from the lava surface, where the contact temperature is

defined as the temperature at the interface between wax or lava and the ambient. Similar to the traditional Peclet number, Π represents a ratio of a characteristic flow rate downstream to a characteristic thermal diffusion rate at the surface of the flow [Fink and Griffiths, 1990, Eq. 11]. Now, the formula for Ψ can be written as:

$$\Psi = \Pi\tau_s(\theta_s) \tag{3}$$

Calculated Ψ is a function of instantaneous effusion rate, time, and temperature of the erupted wax. Additional formulas and derivations can be found in Fink and Griffiths [1990] and the supplementary datasets of this work. Fink and Griffiths [1990] observed that flow behavior and morphology differed across a continuum of Ψ regimes. Five flow regimes corresponding to discrete Ψ ranges were observed. Those regimes which correspond to observed morphologies, from high to low Ψ, are: No Crust, Levees, Folds, Rifts, and Pillows (Fig. 2) [Fink and Griffiths, 1990, Fink and Griffiths, 1992; Gregg and Fink, 2000]. Transitional morphologies are also observed, demonstrating that the morphologies are produced on a continuum. These morphologies are analogous to flow morphologies and surface textures observed in nature, with the exception of No Crust [Fink and Fletcher, 1978; Fink and Griffiths, 1990, Fink and Griffiths, 1992; Gregg and Fink, 2000]. 'Levees' are analogous to channelized flow morphology, 'Folds' are channelized flows with an extensive surface crust that has undergone compression producing ripple or folded surface textures. On the other hand, 'Rifts' represent flows where plates of wax (lacking folded textures) have solidified, but rupture – *rift* – apart and hot wax fills the rift, while 'Pillows' are analogous to pillow basalts or smooth pāhoehoe. A full summary of these morphologies is provided in Fink and Griffiths [1990]. Crustal extent and strength increase with decreasing Ψ. In summary, Ψ is a powerful tool that relates the morphology of a flow to its cooling and flow regimes.

In general, previous studies either limited their experiments to constant eruption conditions or did not account for how varying effusion rates with time affected propagation rate and morphology [e.g., Baloga and Pieri, 1986; Griffiths and Fink, 1992; Blake and Bruno, 2000; Cashman et al., 2006; Garry et al., 2006]. Recently, the use of PEG wax experiments and Ψ has been invoked to understand the role of unsteady eruption conditions and its effects on inflation in the context of large igneous provinces, such as the Deccan Traps, and to understand dome structure and stability [Rader et al., 2017; Lev et al., 2019 and references therein]. These experiments targeted lower Ψ regimes ($\Psi < 15$) where inflation is more likely and is thought to be more applicable to the processes hypothesized to occur during the emplacement of extensive lava flows within large igneous provinces [Rader et al., 2017].

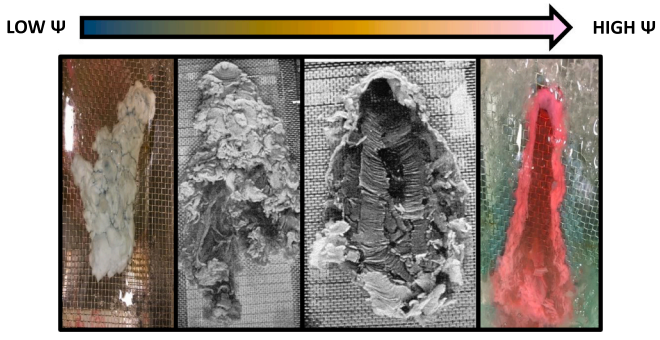

Fig. 2. Four primary morphologies observed by Fink and Griffiths [1990] and their relation to Ψ. A fifth morphology (No Crust, not pictured here) was observed beyond Levees and may be appropriate to some systems. Crustal extent and strength decreases from low to high Ψ values. Approximate Ψ value ranges of morphologies observed in our experiments are as follows: Pillows (≤2); Rifts (~4–12); Folds (~15–29); Levees (~34–54); No Crust (>55). Values in-between these classifications frequently result in transition morphologies, defined here as morphologies that form contemporaneously. Blurriness in colorized lab images due to ice. Image adapted from Fink and Griffiths [1990] and Peters et al. (2021). New, colorized experiments were conducted by the authors.

Here, we expand the Rader et al. [2017] work and demonstrate that variations in eruption rate at the vent control how mass is transported, distributed, and stored within a flow and where the flow is likely to divert that mass to propagate or thicken the flow, which has consequences for mode of emplacement. At the same time, we relate the full spectrum of Ψ regimes and a wide range of eruption rates to the modes of emplacement investigated here. As stated above, effusion rates vary over the course of a volcanic eruption with many eruptions initiating with a rapid spike in effusion rate which then decreases exponentially in time [e.g., Walker, 1973; Wadge, 1981; Tarquini and d'Michieli Vitturi, *2014*]. However, effusion rate can also spike, sometimes multiple times, during this decreasing phase [e.g., Wadge, 1981; Bonny and Wright, 2017]. In order to simulate these fluctuations in the lab, we constructed simplified models of eruption time-series, focusing on sudden increases and sudden decreases in eruption rate. By doing so, we are able to ascertain which types of eruption rate fluctuations are favorable to different emplacement modes – flow stacking via resurfacing, flow propagation by breakouts and/or tube formation, and/or flow thickening by inflation – and how those modes ultimately affect propagation rate and total area covered by a lava flow.

2. Methodology

2.1. Experimental setup and physical parameters

To study the effects of unsteady eruption rates at the vent on the propagation and morphology of lava flows, we performed 120 laboratory analogue experiments. The experiments were conducted in a plexiglass tank with a 60 × 60 cm base (Fig. 3). This tank was placed on a non-adjustable apparatus with a fixed slope of 0°. The flat floor of the tank was fitted with a 0.1 cm thick metal mesh at 0.4 cm grid spacing to prevent slipping at the base of the flows [Fink and Griffiths, 1990, Fink and Griffiths, 1992; Gregg and Fink, 1996, 2000; Blake and Bruno, 2000]. A programmable, peristaltic pump was connected to the base of the tank via a 1-cm diameter latex rubber hose and metal attachment with a 1-cm opening secured to the base of the tank. We used pharmaceutical grade polyethylene glycol (PEG) 600 wax to simulate lava flow emplacement. The kinematic viscosity of the wax is approximately $\sim 10^{-4}$ m^2/s at room temperature and can increase by ~60% as it approaches its solidification temperature. The solidification temperature of the wax was determined to be 18.4 °C. In order to determine the effects of unsteady vent conditions across a variety of eruption regimes, a range of Ψ values from very low to very high (1–70) corresponding to all five morphologies observed by Fink and Griffiths [1990] were tested. Care was taken to avoid running experiments with Ψ values associated with transitional morphologies, although some transitional behavior and morphologies were observed. In the laboratory, instantaneous Ψ was varied by adjusting instantaneous eruption rate and wax temperature, which in turn varied the advective time scale and timescale of wax solidification. For condition 1, experiments in all Ψ regimes were erupted initially from 1 to 6 cm^3/s changing by 1 cm^3/s increments and decreased by a factor of two during the either 10 or 50 s pulse (a step-wise decrease). For condition 2, experiments in all Ψ regimes were erupted initially from 0.5 to 3 cm^3/s changing by 0.5 cm^3/s increments and increased by a factor of 2 during the either 10 or 50 s pulse (a step-wise increase). Average, or mean, Ψ for an experimental run was calculated using the instantaneous eruption rates, eruption temperature, and eruption durations.

Ψ is sensitive to temperature of both the ambient environment and the wax. The temperature of the wax and chilled bath was measured to a tenth of a degree. The tank was filled with a fresh-water bath maintained near 0 °C. A 0.5 °C increase in ambient (water) temperature introduces a 7% error in instantaneous Ψ. As a result, the water bath was kept

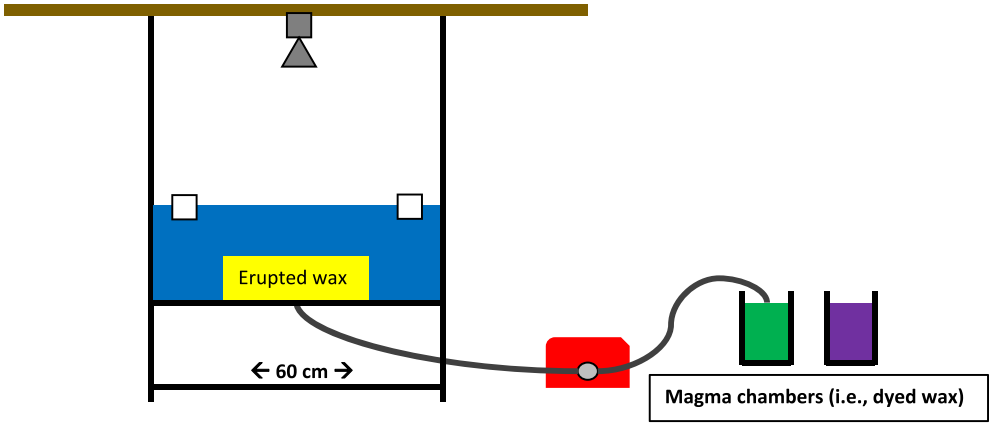

Fig. 3. Schematic of laboratory setup, including plexiglass tank, programmable pump, and reservoirs of wax. White squares and blue shading represent ice and water, respectively. The tank sat atop a flat, fixed apparatus and was filled with water chilled to 0 °C by crushed ice. A camera was placed directly overhead to record the experiments. A 1-cm hose connected the base of the tank with the programmable pump. The same hose fed into reservoirs of wax dyed different colors to simulate a magma chamber. Tank base measures 60 × 60 cm. A 4 mm spaced steel mesh at the bottom of the tank prevents slip conditions. Hole in the center of the base of the tank represents the vent and the center of the eruption. (For interpretation of the references to color in this figure legend, the reader is referred to the web version of this article.)

<0.4 °C for every experimental run. A 0.5 °C difference in Ψ erupted wax temperature produces a 10% error in instantaneous Ψ. However, wax was not erupted until it was +0.1 °C above its erupted temperature to account for heating loss in the tube. PEG wax was dispensed into two 1000 cm^3 beakers to simulate a magma reservoir and heated or cooled to a desired temperature (19.6–32.1 °C from low to high Ψ, respectively). The two batches of wax were dyed pre-experiment using food coloring in order to better visualize the flows and distinguish different stages of the eruption.

In order to simulate unsteady vent conditions, the experiments were divided into two simple conditions (Fig. 4). Conditions 1 and 2 feature 60 experimental runs each for a total of 120 experiments. Condition 1 is characterized by a nearly instantaneous decrease in the eruption rate, also referred to as a decreasing eruption. Condition 2 represents a nearly instantaneous increase in eruption rate, also referred to as an increasing eruption. Hereafter, condition 1 and 2 will be referred to as 'Decreasing (eruption rate)' and 'Increasing (eruption rate)'. The period of time representing the second stage of increase or decrease in eruption rate is termed the *pulse*. The length of the pulse for our experiments was either 10 s (short pulse) or 50 s (long pulse). Depending on the condition, the eruption rate during the pulse was either half the initial eruption rate (for condition 1 / decreasing) or double the initial eruption rate (for condition 2 / increasing). There was a brief (~1 s) pause at the start of each pulse to switch the rubber hose from one wax reservoir to another of the same temperature but different color. This pause accounted for <1% of the experimental run time and had no visible effect on morphology or emplacement nor was it discernible in the datasets. Previous experiments found that pauses of 15–120 s were required to

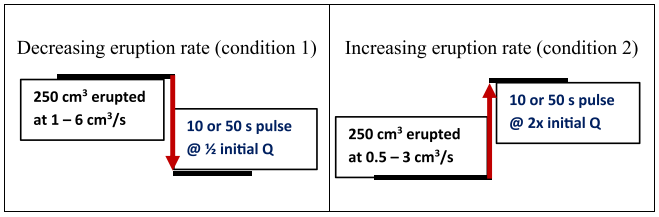

Fig. 4. Schematic of experimental design. The experimental design consists of two conditions corresponding to a stepwise decrease in eruption rates (condition 1) and a stepwise increase in eruption rates (condition 2). For condition 1, the eruption rates were halved from 1 to 6 cm^3/s to 0.5–3 cm^3/s for either 10 or 50 s. For condition 2, the eruption rates were doubled from 0.5 to 3 cm^3/s to 1–6 cm^3/s for either 10 or 50 s. The volume erupted during the pulse differs depending on the duration and eruption rate. These stepwise changes in eruption rate simulate a period of time in a volcanic eruption when the flow rates are decreasing or increasing.

impact experiments [Rader et al., 2017]. At the start of the pulse, some volume of wax (~ < < 75 cm^3, which is the volume of the rubber hose) of the previous color could be erupted at the rate of the pulse, although we attempted to mitigate this by removing the hose from the 1st reservoir of wax while the pump continued to run at the initial flow rate in order to empty the hose before changing reservoirs and flow rate. After the pulse, the experiment ceased. For each experimental run, a volume of 250 cm^3 of dyed PEG wax was erupted into the water filled tank at an initial rate of 1–6 cm^3/s during the first stage of the experiment prior to the pulse. The duration of the first stage of the eruption depended on the eruption rate and ranged from 250 – ~40 s at 1–6 cm^3/s for condition 1 and 500 - ~83 s at 0.5–3 cm^3/s for condition 2. The eruption of this initial volume allowed the flow to mature before the onset of the pulse stage. The eruption rate was then adjusted after the initial eruption of 250 cm^3 of wax. The volume of wax erupted during the pulse was dictated by the flow rate and duration of the pulse, and ranged from 5 to 300 cm^3 for all combinations described here. In addition, the total volumes of experiments differ slightly between conditions 1 and 2. The details of all experimental conditions, including total volume erupted, are compiled in Table 1. Flow depth was measured by taking three separate measurements of the flow by either inserting a ruler and/or cross-sectioning the flow and measuring its thickness. When discussing flow dimensions, it is also important to note that flow depth and deposit thickness have the same value when the deposit is only one flow unit thick and produced by the same eruption. In this study, we define the flow depth as the thickness of the flow deposit after the eruption has ceased as the flows represent one continuous eruption.

2.2. Image analysis & flow propagation

Experiments were either photographed and/or recorded using a Nikon digital camera and Apple iPhone 6S. The camera was positioned for videography on a tripod adjacent to the tank. Overhead photographs were collected at the end of each experimental run, typically no sooner than 60 s after the experiment had ceased and after the wax stopped flowing and solidified. In order to collect morphometric data on the flows, we used Tracker and ImageJ for quantitative analyses. Tracker is an open-source video analysis and modelling tool built in Java and utilized by introductory physics courses [Brown, 2009; https://physlets.org/tracker], and was used to track the flow fronts or flow area with time. ImageJ is an open-source Java-based image processing program [Abramoff et al., 2004], and was used to calculate the final area of the flows and the area of the flow that had been resurfaced.

In order to track flow propagation, the area of the flows was measured just before the pulse and after the cessation of the experiment using Tracker and Image J. This produced three data points per

Table 1
Provided are the independent and dependent variables for decreasing eruption rate (condition 1) and increasing eruption rate (condition 2). The water temperature for the bath for all experiments was 0 °C. For example, experiment 15 (pictured in Fig. 6 – condition 1, high Ψ, short pulse) has a mean Ψ of 44.9, an eruption temperature of 27.2 °C, instantaneous eruption rate of 4 cm^3/s at the start of the experiment, and a pulse duration of 10 s. Other values are also listed related to ambient and wax properties in the supplementary dataset. For a complete list of every experiment, see dataset (https://doi.org/10.48349/ASU/LTWBGY).

Table of Input and Output Values							
	Ψ Regime (numerical mean Ψ value)	Pulse Duration (s)		Erupted Wax Temperature (°C)	Mean Eruption Rate (cm^3/s)	Pulse erupted volume for 10, 50 s (cm^3)	Total erupted volume (cm^3)
Decreasing eruption rates (condition 1)	Very High (67–70.5)	10	50	28.7–31.1	~1.0–5.50	5–30, 25–150	255–400
	High (41.2–45)	10	50	26.7–28.7			
	Intermediate (20–21.5)	10	50	24.2–25.6			
	Low (7.6–8.4)	10	50	22.0–22.9			
	Very Low (0.9–1)	10	50	19.6–20.0			
Increasing eruption rates (condition 2)	Very High (70.8–76)	10	50	29.6–32.1	~0.5–4.25	10–60.0, 50–300	260–550
	High (45.4–49)	10	50	27.5–29.6			
	Intermediate (21.2–22.9)	10	50	24.6–26.2			
	Low (8.1–8.8)	10	50	22.3–23.2			
	Very Low (1–1.1)	10	50	19.8–20.1			

experiment (including the flow area at the start of each experimental run, which is 0 cm^2) allowing for the examination of flow area with respect to time. When coupled with additional observational data (i.e., reviewing video recordings, qualitative evaluation, cross sectioning, and final depth measurements), it is possible to assess when the emplacement modes are happening relative to eruption timing and flow propagation.

2.3. Scaling

The use of nondimensional variables in analogue experiments is critical to ensuring that the processes observed in the lab are analogous with those in nature. We calculated the non-dimensional Ψ value using eqs. (1 and 2) derived and adjusted by Fink and Griffiths [1990] and Gregg and Fink [1996]. Ψ is a ratio of the rate of heat transfer by diffusion (i.e., diffusion upward through the surface of the flow) to the rate of heat transfer by advection (i.e., forward propagation of the flow). Therefore, a lower Ψ indicates a stronger crust, while a higher Ψ denotes a weaker crust. Included in Ψ is Π, the modified Peclet number, which is a ratio of the rate of advection and the rate of a diffusion of a temperature within the flow. Derivations and further discussion of Ψ and its associated input variables are found in Fink and Griffiths [1990] and Gregg and Fink [1996]. The relationship between Ψ and crust is such that higher Ψ values result in a thinner, weaker crust. In wax experiments, this can be identified qualitatively as a crust that is translucent. Lower Ψ values produce a stronger, coherent crust which manifests as opaque crust in analogue wax experiments. In addition to factors such as eruption rate, the competence and extensiveness of a surface crust can exert a control on flow emplacement and flow morphology.

3. Qualitative observations: decreasing (condition 1) and increasing (condition 2) eruption rates

In the following subsections, we detail the qualitative insights gained from the 60 experiments performed at a decreasing eruption rate (condition 1) and the 60 experiments at an increasing eruption rate (condition 2). Mean Ψ is calculated using the instantaneous eruption rate, temperature, and duration of each eruption stage and experimental run. For the sake of brevity, we group Very High Ψ (67–76; No Crust) and High Ψ (41.2–49; Levees/channelized) into one section and Low Ψ (7.6–8.8; Rifts) and Very Low Ψ (0.9–1.1; Pillows) into one section for all conditions. Morphologic designations come from previous studies and function as a way to describe the general regime under which each experiment was performed, although the designations may not reflect the subtleties observed in this study [e.g., Fink and Griffiths, 1990, Fink and Griffiths, 1992; Gregg and Fink, 1996, 2000]. The qualitative observations below are followed by quantitative classification of the flows and direct comparison between decreasing and increasing eruption conditions. Examples of flows produced during decreasing and increasing eruption conditions are depicted in Fig. 5.

3.1. Decreasing eruption rate (condition 1) – qualitative descriptions

3.1.1. Very High and high Ψ regime ($\Psi \geq 41.2$)

For the purposes of condition 1 qualitative descriptions, high eruption rates (Q) refer to mean eruption rates >4 cm^3/s and low Q refer to mean eruption rates <2 cm^3/s. The very high and high Ψ regime corresponds to the no crust and levee morphologies, respectively, observed in the lab in previous studies [e.g., Fink and Griffiths, 1990, Fink and Griffiths, 1992; Gregg and Fink, 1996, 2000]. A total of 24 experiments were conducted at 'very high' and 'high' Ψ values, with 12 experiments conducted under each regime. Of those 12 experiments, half featured the short (10 s) pulse and the other half featured the long (50 s) pulse. Fig. 5 (Part A) provides an example of flows erupted under these conditions.

At the onset, the flows erupted approximately axisymmetric in plan form. Wax typically remained liquid with no appreciable crust forming for the first few seconds. Depending on the initial eruption rate (Q), the crust formed closer to (low Q) or farther from (high Q) the vent. Crust also varied in thickness and extent such that high Q favored thinner patchier crusts, which were susceptible to failure via fracturing, foundering, and rifting. Low Q favored thicker, extensive crusts, less prone to failure. As the flow propagated away from the vent, the local flow rate dropped and the flow front started to solidify and circumferential levees formed at the flow front. The crust was generally translucent during this stage.

The flow rate was dropped to half the initial eruption rate to initiate the pulse. At the onset of the pulse the flow remained mostly molten. At high Q, this pulse of wax encountered no crust and propagated forward by either pushing the still molten wax from the initial stage forward or channelizing into sinuous pathways. At low initial Q, the pulse encountered a thin, translucent crust and flowed beneath it radially away from the vent. Because the same volume of wax was erupted in the first stage for all experiments, low-Q experiments were longer in duration, allowing more time for crust development during the first stage of the eruption. Thus, the pulse of wax during the second stage would either rupture through the thin crust (10 s pulse), mobilize unsolidified wax which would either rupture the crust or create breakouts (10 and 50 s pulse), or disrupt levees at the flow front and advance the flow (50 s pulse). After solidification, the flows rarely preserved a smooth, featureless morphology.

3.1.2. Intermediate Ψ regime ($\Psi = 20–22.9$)

At the onset, intermediate Ψ-regime flows (Fig. 5b, left panel)

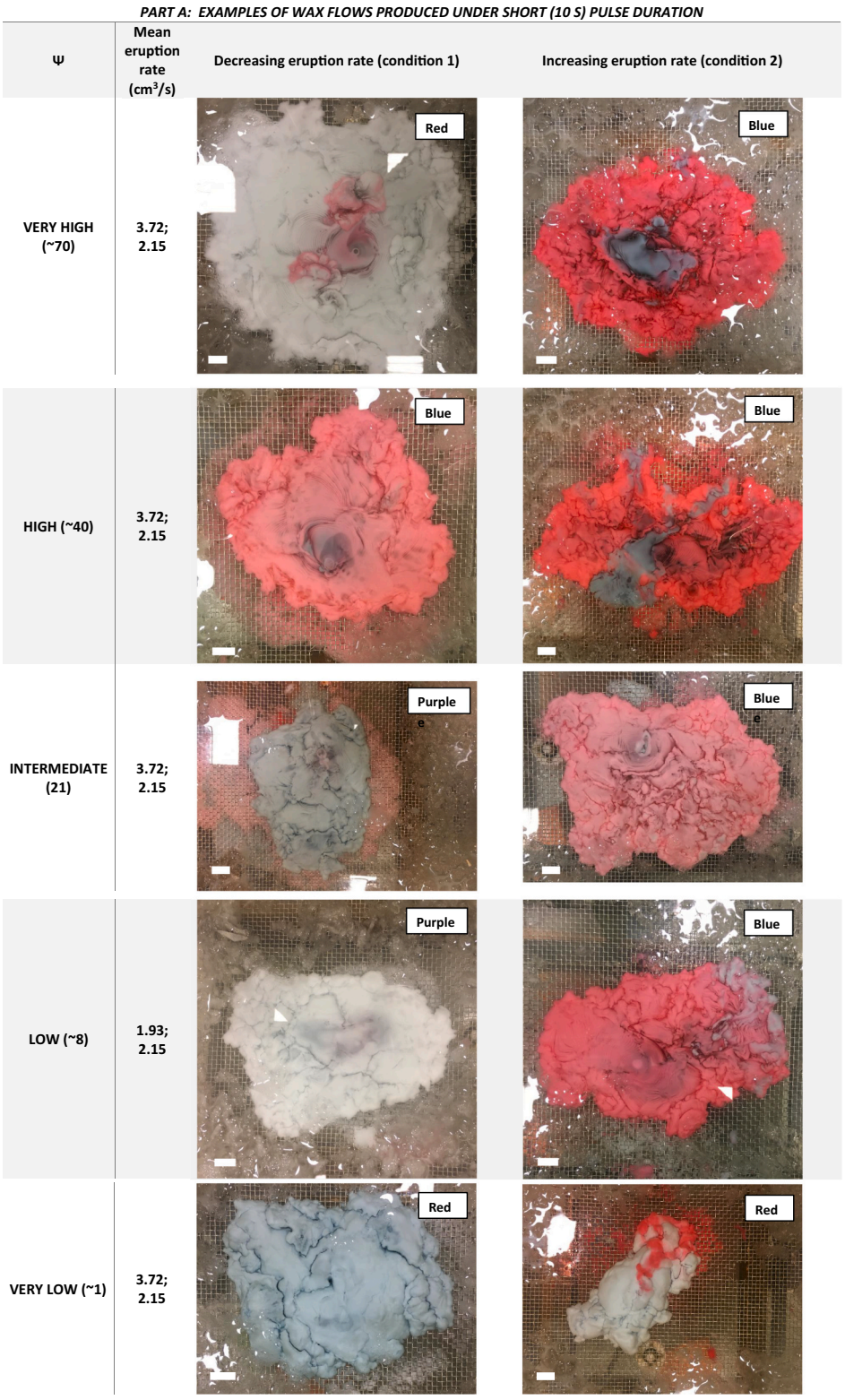

Fig. 5. Images taken of 20 solidified wax flows produced under either decreasing or increasing eruption rates. White scale bars are 2 cm in each photo. Blurriness is caused by crushed ice. Rectangular glare caused by overhead lights. Flows in the left panels were erupted with decreasing eruption rates and flows in the right panels were erupted with increasing eruption rates. Dark hues of wax color indicate the presence of liquid wax, typically beneath a relatively thin crust. Text boxes in the upper right corner of each flow image denote the color of the wax erupted during the pulse. **(top panel)** A panel of 10 wax flows representing very low ($\Psi \sim 1$) to very high ($\Psi \sim 70$)Ψ under decreasing and increasing eruption rates for short (10 s) pulse durations. **(bottom panel)** A panel of 10 wax flows representing very low ($\Psi \sim 1$) to very high ($\Psi \sim 70$) Ψ under decreasing and increasing eruption rates for long (50 s) pulse durations.

PART B: EXAMPLES OF WAX FLOWS PRODUCED UNDER LONG (50 S) PULSE DURATION

Ψ	Mean eruption rate (cm^3/s)	Decreasing eruption rate (condition 1)	Increasing eruption rate (condition 2)
VERY HIGH (~70)	4.11; 2.57	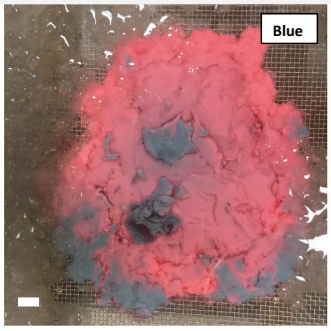	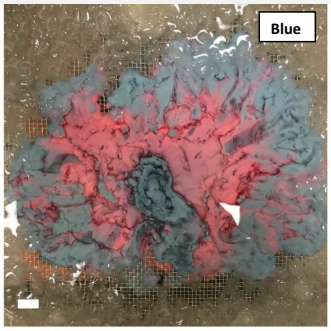
HIGH (~40)	3.11; 2.57	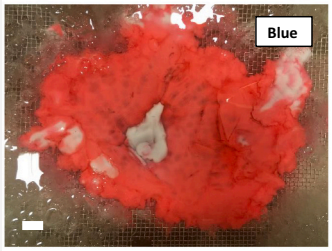	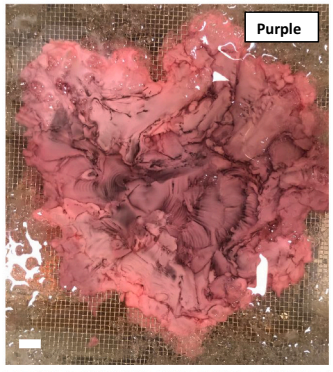
INTERMEDIATE (21)	3.11; 2.57	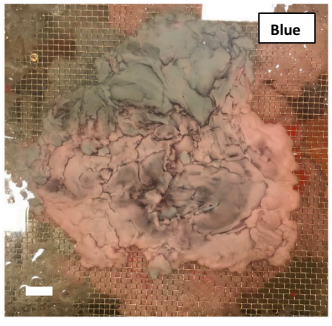	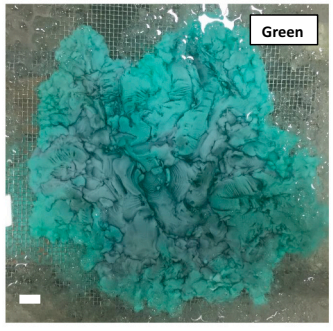
LOW (~8)	3.11; 2.57	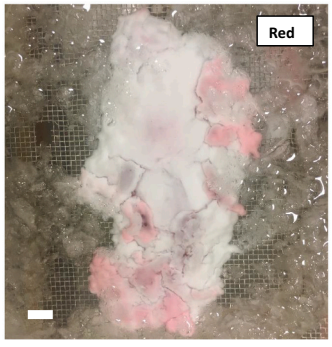	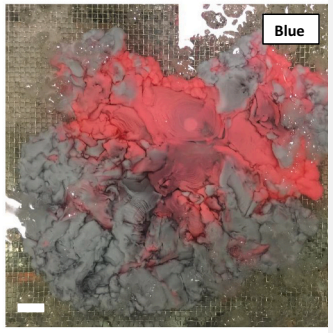
VERY LOW (~1)	3.11; 2.57	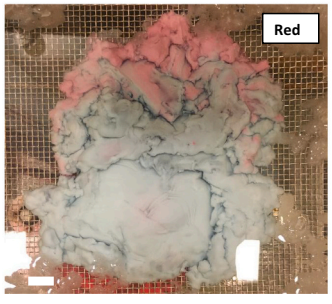	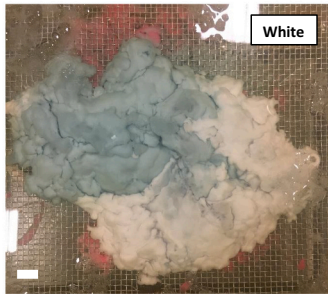

Fig. 5. (*continued*).

erupted asymmetrically. Due to the slightly higher viscosities of the erupted wax (a consequence of lower erupted temperature) relative to the high-Ψ regime, these flows spread more slowly and were thicker. The onset of crust formation was quicker in this Ψ regime. In some flows, folds formed on the flow surface and propagated back toward the vent. Higher eruption rates promoted more radial branches of folding in the flow, while lower initial eruption rates promoted a thicker crust that inhibited fold formation. Overall, the crust was more expansive and thicker than in higher Ψ regimes.

In the second stage of the eruption, the low-eruption-rate pulse, wax spread radially from the vent flowing beneath the crust formed during the initial stage. Although the crust was slightly thicker than in higher Ψ regimes, it remained thin enough to be somewhat translucent. As a result, wax eventually ruptured the crust and oozed out onto the flow surface during resurfacing events. In general, as with previous regimes, the 50 s pulse promoted thicker crusts due to increased time for wax to cool and a drop in local flow rates at the flow front. Thicker crusts tended to more effectively trap the wax erupted during the pulse, and in turn promoted thickening of the flow via inflation and reduced the areal extent of breakouts at the flow front. While an increase in the number of breakouts on the flow surface is observed in conjunction with thicker crusts causing a larger percentage of the flow to be resurfaced, the increase in percentage of resurfacing is an artifact of the smaller final flow areas observed.

3.1.3. Low and very low Ψ regime ($\Psi \leq 7.6$)

A thin, deformable crust formed almost immediately in these flows (Fig. 5, lower panels of Part A). Eventually an extensive, semi-opaque to opaque crust developed covering most of, if not the entire, flow. At lower Q in particular, the development of this crust early in the eruption sometimes prevented an axisymmetric flow plan. The continued injection of wax beneath the crust led to fracturing of the crust into large segments, exposing molten wax and allowing it to flow from beneath the crust through the fractures. Upon interaction with the water bath, this molten wax quickly developed a surface crust. Sometimes, the molten wax carried rafted bits of solidified crust until the molten wax itself solidified.

Although the flow surface was largely solidified shortly after eruption, the initial eruption rate influenced how far the flow propagated from the vent. Breakouts that occurred at the flow margin quickly acquired a pliable crust which then thickened and became stiff. At the lowest Ψ values, flows took on bulbous appearances as lobes of wax analogous to pillow lavas. Higher eruption rates formed longer, larger lobes and lower eruption rates formed smaller lobes. As the eruption progressed, the crust at the lowest Ψ regime thickened and became opaque. The opacity of crust hindered observation of the flow interior. Only the increasing prevalence of breakouts or inflation of the flow was observable.

Due to the thicker, opaque surface crust, the behavior of the low-eruption-rate pulse of wax in the second stage of the eruption was learned not only by observing the flows in action but also by dissecting the flows post-eruption. During the pulse, the newly erupted wax pooled beneath the crust, initially spreading radially although sometimes restricted by thicker crust. As a result, the wax typically exhibited three behaviors listed here from high to low eruption rate: breakout at the flow margin, rupture at a weak point in the crust and spilling onto the flow surface (resurfacing), or accumulation beneath the flow, inflating, rather than propagating, the flow.

3.1.4. Summary of qualitative descriptions

- At high Ψ, the crust is tenuous and exerts less control on flow behavior. Longer pulse durations result in more flow modification, specifically marginal breakouts.
- At intermediate Ψ, the crust is more present and exerts more flow control which promotes flow thickening via inflation. Resurfacing is observed and the percentage of resurfacing is higher than at higher Ψ, which is partly a result of the smaller final flow area.
- At low Ψ, the crust is coherent and insulating which promotes flow thickening via inflation and resurfacing.
- At higher mean eruption rates, the crust is less resilient and flow advance is quicker. Breakouts, both surficial and marginal, are more vigorous.
- At lower mean eruption rates, the crust is more resilient and the flow advance is slower. Breakouts are, correspondingly, slower and less frequent.

3.2. Increasing eruption rate (condition 2) – qualitative descriptions

3.2.1. Very high and high ψ regime ($\Psi \geq 45.4$)

For the purposes of condition 2 qualitative descriptions, high eruption rates (Q) refer to mean eruption rates >3 cm^3/s and low Q refer to mean eruption rates <1.5 cm^3/s. In condition 2, the wax was erupted at a lower initial Q than condition 1 and after a fixed volume was erupted (~250 cm^3), the eruption rate was increased to double the initial Q. Fig. 5 (Part B) provides examples of flows erupted under these conditions. From the onset, the wax flowed radially from the vent producing an approximately axisymmetric flow. Some distance from the vent levees developed around the circumference and a crust started to form across most of the flow. Note that because the first stage erupts a fixed volume, stage one in condition 2 lasts longer than stage one in condition 1. As a result, flows created by condition 2 display a systematic behavior of lower Ψ regimes closer to the vent relative to condition 1. Crusts formed during the initial stage of the eruption were generally translucent and extensive in area.

The second stage of the eruption – the high-flux pulse – created different flow regimes not observed in condition 1. The pulse of molten wax initially spread radially from the vent, and then eventually ruptured any crust and/or displaced any molten wax near the vent. This process occurred for all values of Q. If a more extensive crust was present some distance from the vent (moderate to high Q), the fresh molten wax would either flow over the crust, flow under the crust, and/or disrupt the crust by rupturing it and tearing it apart. In runs with a more extensive crust near the vent (low Q), the resurfacing and/or disruption of the flow was less extensive and less disruptive such that most of the fresh molten wax flowed beneath this crust. Wax that flowed under the crust ultimately erupted at the flow front as marginal breakouts, sometimes disrupting pre-existing levees, expanding the flow front and increasing the areal extent of the flow rapidly.

For long duration pulses (50 s) irrespective of eruption rate, molten wax tended to develop preferred pathways that sometimes developed into tubes in the presence of an extensive, coherent crust. The fresh molten wax issued during the pulse had a longer runout distance from the vent than the preceding flow and formed a surface crust farther away from the vent.

At higher Q, the entire flow was disrupted by the pulse and the flow was more axisymmetric due to the ability of the wax of the pulse to disrupt the crust and expand radially at the flow front, sometimes resurfacing the entire flow. In fact, the wax erupted in the second stage more resembled an ideal very high Ψ (no crust) regime than the initial stage of the eruption. This is due to partial insulation of the pulse wax by a thin crust (when present) and the decreased flow times due to the higher eruption rate. At lower Q, the flow was more asymmetric due to a stronger crust from the initial eruptive stage which tended to solidify as 'levees' at the flow margin which stopped radial flow and diverted the pulse wax. This hindrance of radial flow and diversion of the pulse wax by the flow margin limited the ability of the pulse of molten wax to disrupt the flow and spread radially at the flow front.

3.2.2. Intermediate Ψ regime (Ψ = 21.2–22.9)

Wax initially erupted radially from the vent but rapid and widespread formation of a crust usually prevented true axisymmetric, radial flow. The crust buckled as the faster flow rate near the vent encountered the slower localized flow rate at the distal margins of the flow, forming compression ridges, or folds. The decreasing local velocities far from the vent led to locally lower Ψ regimes and corresponding morphologies, progressing from folds to rifts, rift-pillows, to pillows with increasing distance from the vent.

The movement of the pulse wax was restricted by the competent crust and generally tended to flow beneath it, commonly leading to rupturing of the pre-existing crust. At higher Q, if the crust was ruptured, the pulse of wax would destroy or overprint the pre-existing flow via a wholesale resurfacing event. At lower Q, a rupture of the crust was gentler, leading to wax oozing out from fractures. At very low Q, this rupture and resurfacing process resembled that observed for very low Ψ (pillow or pāhoehoe morphology) observed in condition 1, with small bulbous lobes oozing from the fractures. Wax that remained flowing beneath the pre-existing crust tended to erupt at the flow margin, pushing any remaining molten wax forward as well. For long pulses, the effects were more extensive, with the areal extent of the flow doubled during every 50 s pulse in this regime even though the extruded volumes were roughly 1/6 to ½ of the total volume erupted (Fig. 5 Part B).

3.2.3. Low and very low Ψ regime (Ψ ≤ 8.8)

Although wax initially erupted from the vent radially, the rapid formation of semi-opaque to opaque crust typically resulted in nonuniform propagation of the flow front. Wax readily formed a crust at the flow front and as the crust strengthened, the continued flow of wax from the vent would sometimes rupture this crust. The flow would rift, rafting portions of the crust apart. Other times, the crust would fracture along a rift margin and wax would push the crust up and ooze out over the pre-existing surface crust. This rupturing frequently resembled a precursor to the bulbous growth usually associated with the 'pillow' morphology. As the wax continued to flow away from the vent, the flow transitioned to lower Ψ morphologies (i.e., pillows or smooth pāhoehoe).

For the lowest Ψ values, the thicker, more rigid crust retarded the spreading of the flow, promoting fewer preferred pathways (Fig. 5, Part B lower panels). In some runs, transportation of wax to the flow front, and thus the propagation of the flow front, was halted until the pulse. In other runs, the flow would propagate forward via bulbous breakout lobes. These breakouts most resemble pāhoehoe lavas in the field, with a lobe of wax erupting from a fracture in the crust, forming a thin crust, and oozing onto the flow surface. At high Q, the processes of fracturing the crust and forming lobes was more vigorous. At low Q, the rate of these processes was slower, although the value of Q did not appear to have any effect on whether these processes occurred or not.

There was a stronger impact by the duration of the second stage (pulse) of the eruption at lower Ψ. In general, when the molten wax erupted during the high-Q pulse, the crust over the vent remained intact containing the flowing wax beneath it. Therefore, disruption of the crust tended to occur away from the vent. The pulse of wax flowed less vigorously from any ruptures in the crust. For the short pulse, the limited volume of fresh, molten wax tended to flow beneath the crust and erupt at the flow front via small-scale toes. For flows erupted at lower Q, the thicker crust retarded the effects of the pulse further, usually leading to a thickening of a flow via inflation as wax pooled beneath the crust.

In the lowest Ψ regime, the pulse of material either pushed the flow surface upward or forced the wax through limited fracturing of the crust which produced bulbous lobes. For flows erupted at lower Q, the thicker crust retarded the effects of the pulse, such that the wax tended to erupt from a point of crustal weakness at the flow margin, propagate some distance until the formation of a crust retarded its own progress. However, the preferred pathway created by this breakout would continue to supply molten wax to this region of the flow which could promote more breakouts. Breakouts through the preexisting crust during the long pulse were usually sustained, with molten wax using this preferred pathway until either the flow ceased and/or another more ideal pathway developed. This fresh wax oozed out sometimes as independent lobes and other times as narrow streams of flow. These tended to increase the areal extent of the flow in one or more directions.

3.2.4. Summary of condition 2 qualitative descriptions

- At high Ψ, the crust is tenuous and exerts less control on flow behavior. Longer pulse durations result in more flow modification, specifically voluminous and widespread marginal breakouts.
- At intermediate Ψ, the crust is more present and exerts more flow control which promotes flow thickening via inflation. However, significant crust disruption during the pulse – especially long duration – is still observed usually in the form of resurfacing and widespread breakouts.
- At low Ψ, the crust is coherent and insulating which promotes flow thickening via inflation and resurfacing. During the pulse, resurfacing – in the form of bulbous lobes – produces multiple extrusions at many points in the flow surface.
- At higher mean eruption rates, the crust is more greatly disrupted by breakouts and flow advance is quicker.
- At lower mean eruption rates, the crust is more resilient and the flow advance is slower. Breakouts are, correspondingly, slower and less frequent.

4. Quantitative analysis: effects of decreasing and increasing eruption rates on flow morphology and emplacement

The observational data above for decreasing and increasing eruption rates, conditions 1 and 2 respectively, were further analyzed to identify eruption conditions most favorable to resurfacing, marginal breakouts, inflation, and tubes. Surface morphological terms (i.e., pillows, rifts, levees) were adopted from Fink and Griffiths [1990]. Resurfacing was identified as wax rupturing the crust or overflowing from channels and repaving the preexisting flow surface. Marginal breakouts were an emplacement mechanism identified as wax rupturing crust at the flow margin and advancing the flow. Marginal breakouts were observed during flow emplacement, in video recordings, and in some cases identified by different color wax erupted during the pulse.

Inflation was interpreted as the vertical growth of the flow without rupturing its crust. Through experiments performed prior to the study, we define the standard flow depth as ~0.5 cm on slopes of 0°, which agrees with previous studies [e.g., Fink and Griffiths, 1990; Gregg and Fink, 2000; Garry et al., 2006; Rader et al., 2017]. Therefore, any flow thicker than 0.5 cm is interpreted as having inflated, only if it was also observed to have increased in thickness over time, while simultaneously displaying little to no growth in areal extent and no evidence of meaningful contribution to its thickness via resurfacing.

Tubes are a structural feature and remnant of sub-crustal wax transportation that were observed by slicing through the flows post-experiment and removing them from the chilled bath. Tubes are characterized by sinuous, semi-circular channels carved into the solidified wax. Flows displaying only radial flow and therefore none of the aforementioned complex modes of emplacement were considered to have been emplaced as sheet flows, and are denoted as such. Here we present the results of these analyses by comparing results for conditions 1 and 2.

4.1. Observed emplacement modes

Fig. 6 displays the frequency of the modes of emplacement for decreasing and increasing eruption rates, conditions 1 and 2 respectively. This figure accounts for any experimental run where a particular mode of emplacement was observed regardless of the duration or impact of that mode; if the mode was observed, it was 'counted' here.

4.1.1. Resurfacing

While resurfacing is common across decreasing and increasing conditions, it is a relatively minor process in terms of the percent of the flow area resurfaced (Fig. 7). For decreasing eruption rates, the frequency of resurfacing is dependent on Ψ such that resurfacing occurs more frequently at higher Ψ. Not surprisingly, the frequency and extent of resurfacing increases for long pulses in both conditions when more wax is extruded. For decreasing eruption rates (condition 1), the frequency and areal extent of resurfacing are similar between short (10 s) and long (50 s) duration pulses. The frequency and areal extent of resurfacing are also similar between short duration (10 s) and long duration (50 s) pulses under increasing eruption rates (condition 2). However, the frequency of resurfacing is greater in condition 2 than condition 1 at short and long pulses, respectively. For increasing eruption rates, the areal extent of resurfacing is slightly greater for long pulse durations. The majority of flows (63%) that experienced resurfacing had <15% of their

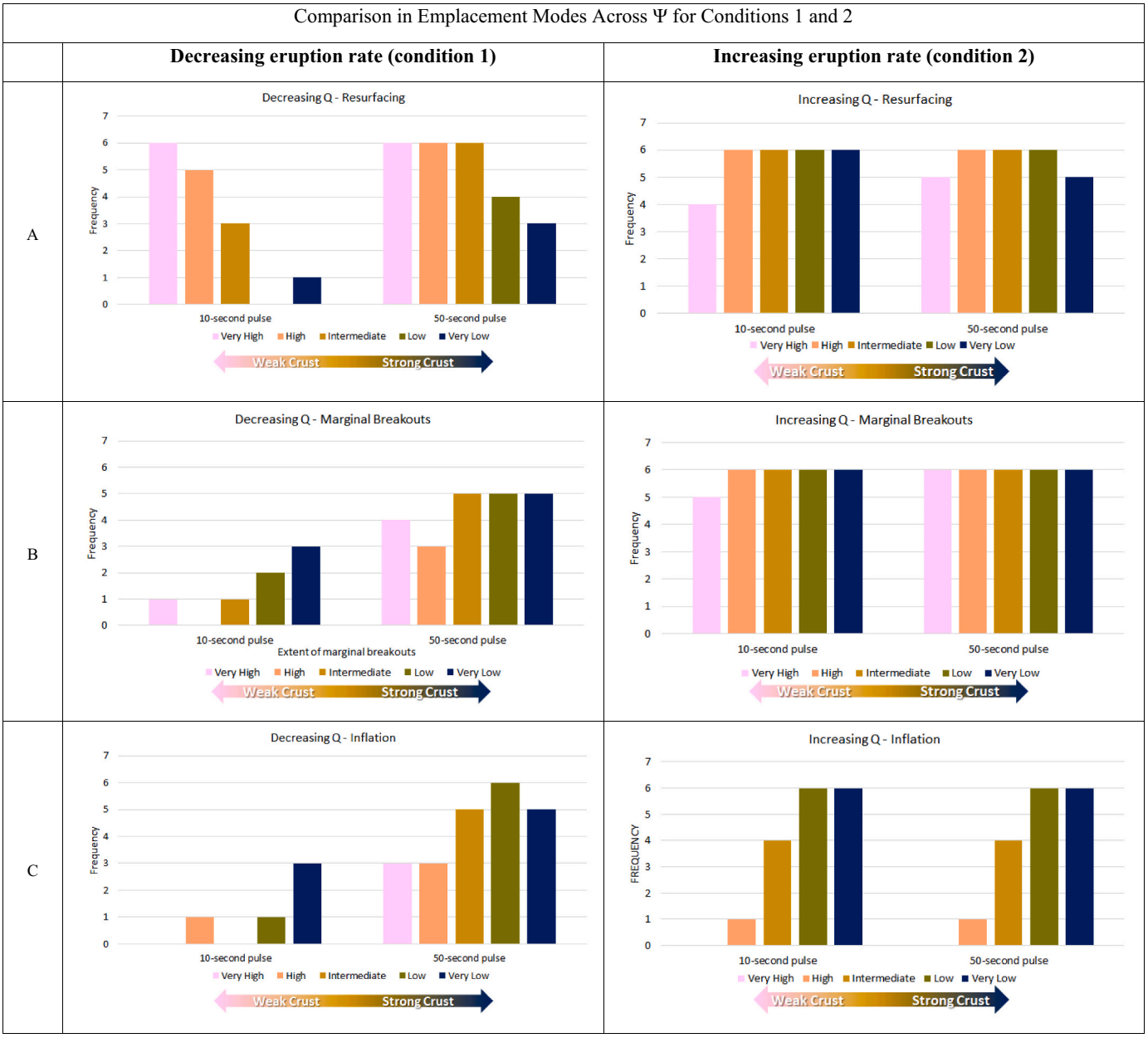

Fig. 6. A comparison of the occurrence of resurfacing, marginal breakouts, inflation, and tubes between conditions 1 and 2 are displayed for each Ψ regime (from very high to very low) and pulse duration. A total of 60 experiments were performed under each condition. (a) In condition 1, resurfacing – which frequently occurred –was dependent on Ψ and pulse duration. For condition 2, resurfacing had no dependence on pulse duration or Ψ. (b) Marginal breakouts were categorized as either local, circum-local, or circumferential. Marginal breakouts were very unlikely to occur for the short pulse. For condition 1, most breakouts were localized, with no dependence on Ψ. In condition 2, a similar of number of experiments experienced localized and circumferential breakouts at the margins. For localized breakouts, a dependence on Ψ is observed with more localized breakouts occurring at lower Ψ. Circumferential breakouts, on the other hand, are more common at higher and intermediate Ψ. (c) In condition 1, inflation was strongly dependent on the pulse duration and less so on Ψ. For condition 2, inflation had no dependence on pulse duration, but was controlled by Ψ. Inflation occurred more frequently for lower Ψ. (d) For condition 1, tubes were the most difficult emplacement mode to produce. The formation of tubes was strongly dependent on pulse length. For shorter pulses, tubes are favored at intermediate Ψ, although they occurred at a similar frequency for all regimes at longer pulse durations. In condition 2, at first glance, *tubes* appear to have some dependence on pulse duration but this could also be a dependence on Ψ at shorter pulse durations. There seems to be some dependence on Ψ morphology, with tubes favoring intermediate Ψ, which correspond with intermediate flow rates. (e) Although sheet flows are rare, they occur in both conditions for short duration pulses but at opposing ends of the Ψ continuum.

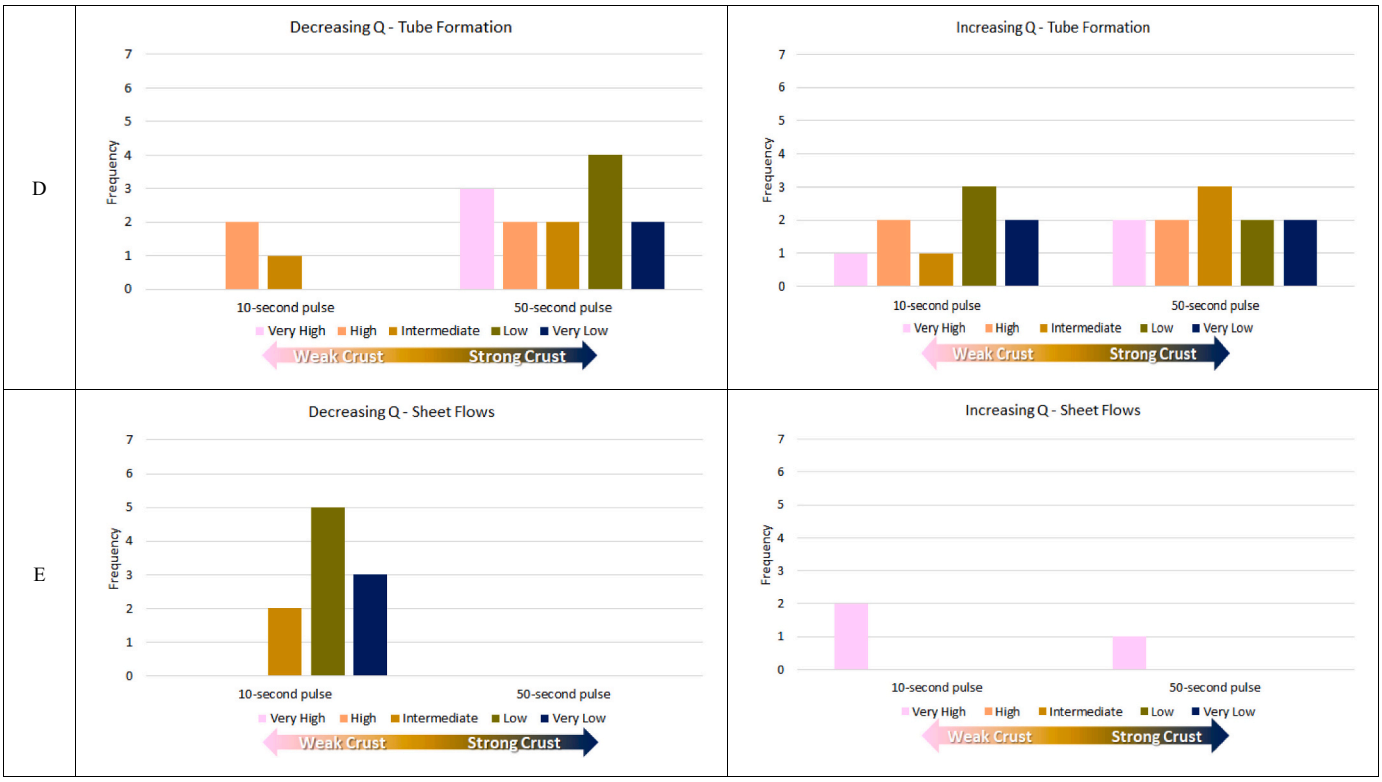

Fig. 6. (*continued*).

areas resurfaced. For increasing eruption rates, the frequency of resurfacing is neither dependent on pulse duration nor Ψ regime, as resurfacing occurs readily across all Ψ values for both pulse durations. Resurfacing is also a relatively minor process for increasing eruption rates (condition 2), although the apparent areal extent of resurfacing is slightly higher than in condition 1 (Fig. 7, right panel). For instance, ~38% of flows (10-s pulse) and ~ 31% of flows (50-s pulse) have resurfacing areas under 5%. A small dependence on pulse duration and the percentage of resurfacing is observed, albeit less than for condition 1. Again, the vast majority of flows have <15% of their flow areas resurfaced: ~66% (10-s pulse) and ~ 79% (50-s pulse). The instantaneous result of the pulse is to prevent much of that erupted material from reaching the active flow front, which has implications for active eruption response. In general, both conditions showed increased areal extent of resurfacing at lower Ψ.

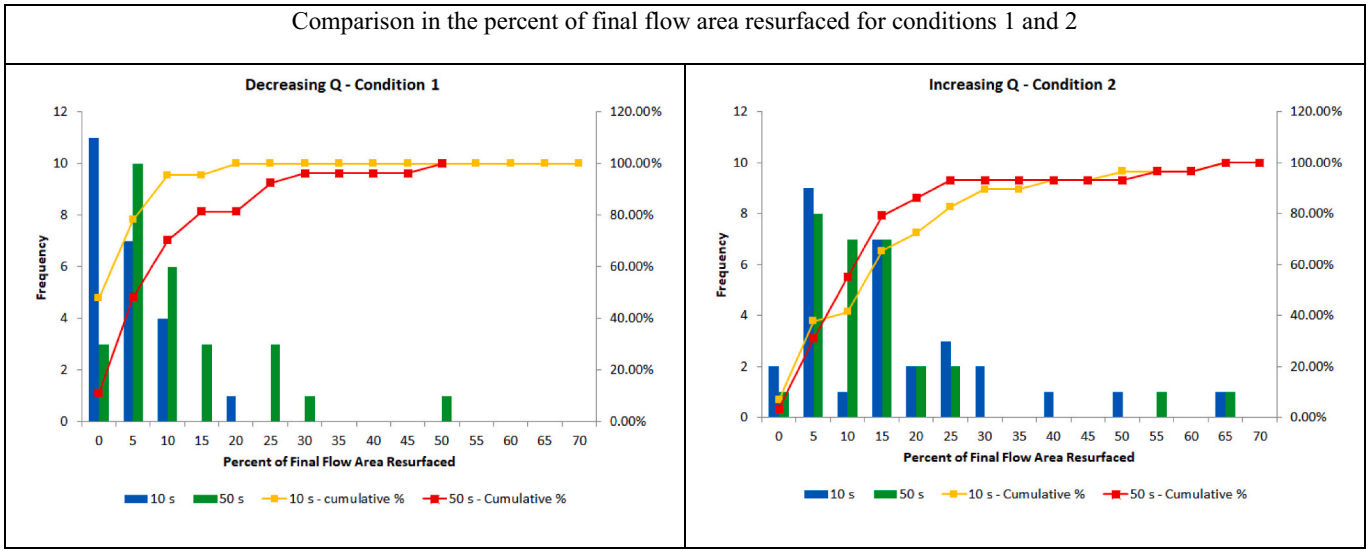

Fig. 7. The percentage of final flow area covered by resurfacing is presented against pulse duration for conditions 1 and 2. Each condition consisted of 60 experimental runs. (Left) In condition 1, most flows where resurfacing is observed experience <20% resurfacing of the final flow area, with many of the flows experiencing <10%. Flows with a 50-s pulse duration had a greater likelihood of increased areal resurfacing. (Right) In condition 2, most flows experienced <25% of resurfacing. However, the majority of flows experienced some degree of resurfacing – 5 to 20% - with a distribution similar for short and long pulse durations.

4.1.2. Marginal breakouts

Marginal breakouts were common, occurring in almost half of the experimental runs for condition 1 and nearly all runs at condition 2 (Fig. 6). Breakouts were characterized as localized (discrete points of eruption), circumferential (multiple points of eruption that comprise the majority of the flow front), or circum-local which is some combination of both (multiple points of eruption that merge to dominate half of the flow front). The term circumferential was adopted due to the roughly radial planform of the flows, although the term widespread is used when discussing flow emplacement later in the text. Marginal breakouts may be minor, manifested as small lobes, or they may be significant and advance the flow front. Breakouts tend to occur in concert with other modes of emplacement, typically following lava emplacement under a crust associated with either inflation or tube formation. The majority of marginal breakouts were localized for decreasing eruption rates (condition 1), although some flows displayed transitional behavior exhibiting both circumferential and localized breakouts (Fig. 6, left panel). There is a dependence on Ψ in condition 1, with the frequency of breakouts increasing with decreasing Ψ – a trend also observed by Blake and Bruno [2000]. There is also a dependence on pulse duration with breakouts occurring almost exclusively in long pulse experiments (Fig. 8). For increasing eruption rates (condition 2), roughly half of the flows experienced localized marginal breakouts while the other half were circumferential. The type of breakout in condition 2 is dependent on Ψ, such that localized breakouts were more common at lower Ψ and circumferential breakouts were more common at high Ψ values. The occurrence of marginal breakouts is not dependent on pulse duration as they occur in every experimental run in this condition. However, the extent of the marginal breakout is dependent on pulse duration (Fig. 8) with localized occurring almost exclusively for short pulses and circumferential breakouts occurring almost exclusively in long pulses.

4.1.3. Inflation

Under decreasing eruption rates (condition 1), inflation was dependent on Ψ, occurring more frequently at lower values and highly dependent on pulse duration with significantly more instances of inflation during experiments with 50-s pulses (Fig. 6, left panel). For increasing eruption rates (condition 2), inflation also had a strong dependence on Ψ and occurred at lower Ψ regimes. In contrast, inflation is not dependent on pulse duration in increasing eruption rates (Fig. 6, right panel), with the same level of occurrence in either scenario.

4.1.4. Tubes

Although tubes occur most commonly for long pulse durations under decreasing eruption rates (condition 1), the total number of tubes observed was higher for increasing eruption rates (condition 2) (compare Fig. 6d, left and right panels). Tubes are more likely to occur for increasing eruption rates (condition 2) than decreasing eruption rates at short pulses. Like inflation, the formation of tubes is strongly dependent on pulse duration and favored in long-pulse experiments. A

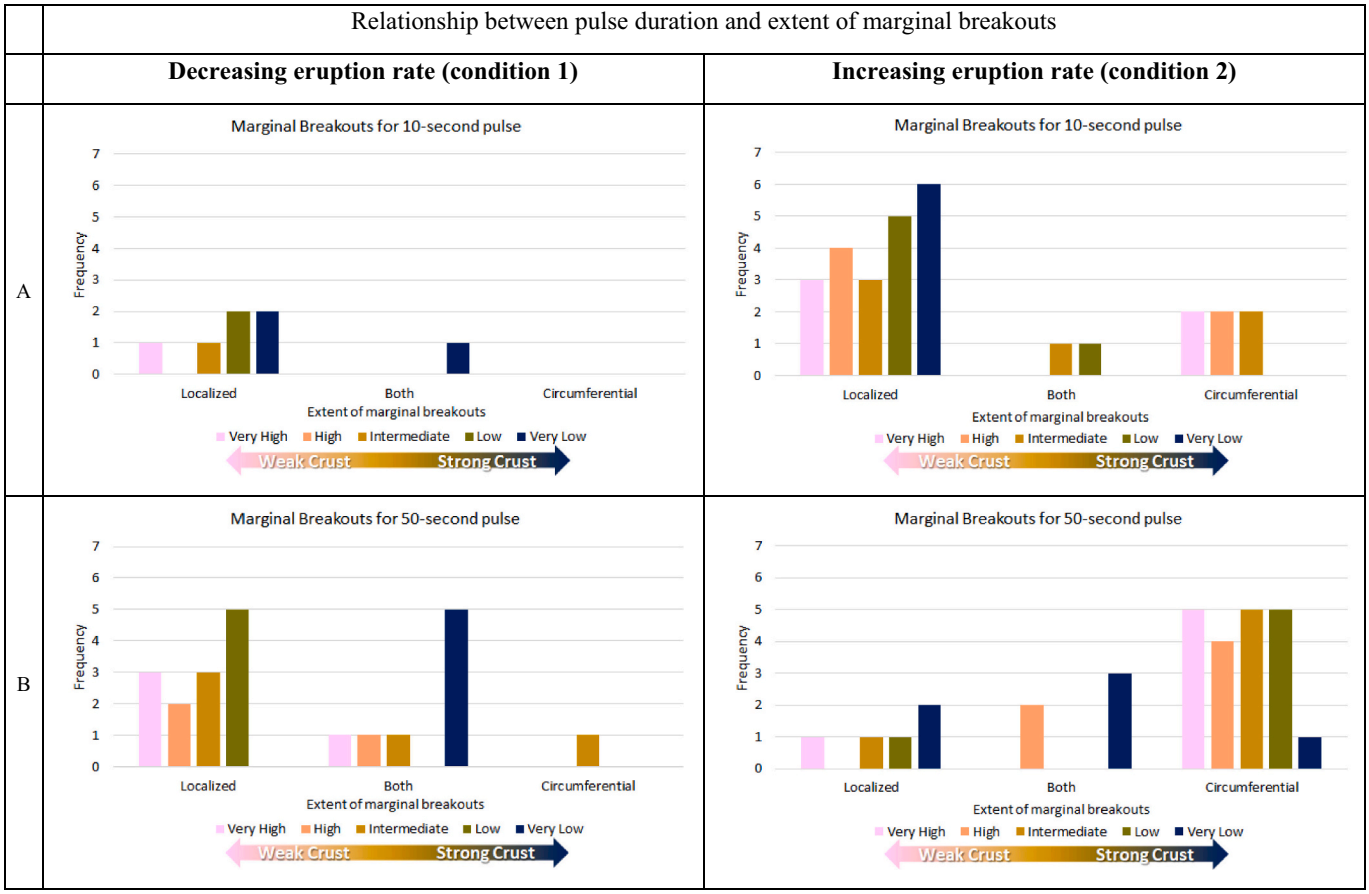

Fig. 8. The relationship between pulse duration and the extent of marginal breakouts, which contribute to flow advancement. Color bars refer to Ψ regime (from very high to very low) which also correspond to crust extent and strength. (a) For the short pulse in condition 1, marginal breakouts were rare and localized. This translates to limited flow advancement. A weak correlation on Ψ is observed. For condition 2, marginal breakouts occur frequently during the short pulse. Although most are localized, as in condition 1, some circumferential, or widespread, breakouts are observed. A dependence on Ψ is observed for localized breakouts, with them being more likely at lower Ψ values. (b) A longer pulse duration resulted in more instance of marginal breakouts in condition 1, although those instances were largely localized. For condition 2, the long pulse resulted primarily in widespread marginal breakouts which corresponded to advancement of the flow front. Dependence on Ψ is less evident for both conditions during the long pulse.

dependence on Ψ is not readily determinable, occurring equally for all Ψ values for long-pulse experiments and too few instances occurring for short pulse experiments. These trends suggest a complicated relationship between pulse duration, Ψ, and tube formation.

4.2. Flow dimensions

The dimensions of the flow are impacted by Ψ as shown by plotting normalized area A against Ψ(Fig. 9). We calculated normalized area as follows:

$$A = \frac{A_{obs} - A_{min}}{A_{max} - A_{min}} \quad (4)$$

The minimum observed flow area was in condition 1 (102 cm^2) while the maximum observed flow area was observed in condition 2 (762 cm^2). Not surprisingly, flows with higher normalized areas tend to have singular emplacement modes and occur primarily at higher Ψ. Flows with the lowest normalized areas occur primarily at Ψ values that are low to intermediate. In both conditions flows erupted with the 50 s pulse generally have greater A relative to their 10 s counterparts, but it is most noticeable for increasing eruption rates (condition 2). This reflects the larger flow areas observed in condition 2 due to the longer eruption duration and slightly larger volume of erupted wax. Thicker, smaller flows are found at lower Ψ, while thinner flows of greater extent (greater A) are produced at higher Ψ.

The difference in erupted volumes between the two conditions varies depending on the pulse duration. For the short duration pulse (10 s), condition 2 flows contain 5–30 cm^3 more volume than in condition 1, a 2–10% increase in volume. For the long duration pulse (50 s), condition 2 flows contain 25–150 cm^3 more volume, or 8–28% increase in volume. Flows erupted in condition 2 are also thinner, even for lower Ψ values where inflation dominates, which suggests the additional volume is increasing flow area, rather than thickening them. This is consistent with marginal breakout observations. The variation in area between flows produced under decreasing (condition 1) and increasing (condition 2) conditions is due to a combination of differences in total erupted volume and in emplacement modes.

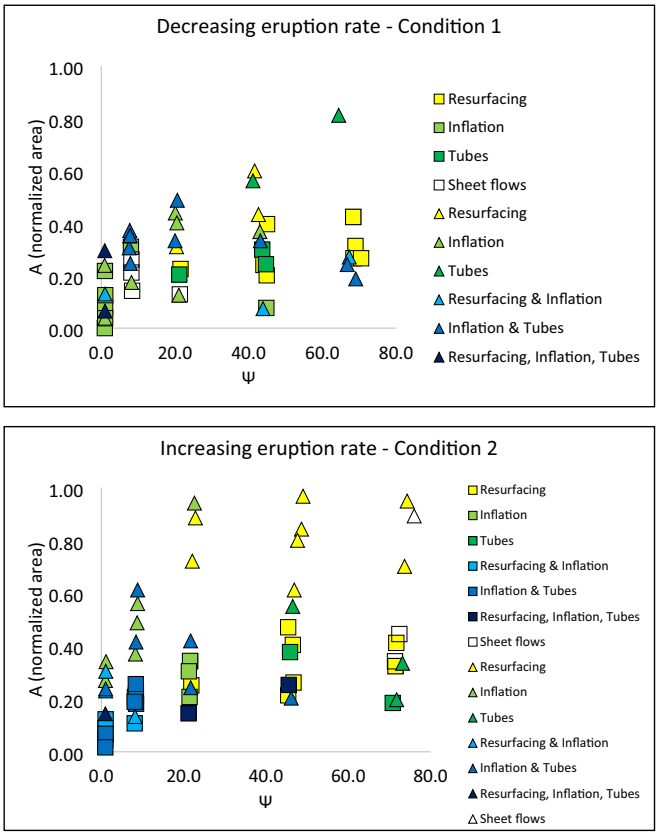

Fig. 9. Normalized area (A), a dimensionless term, vs. Ψ. Symbols indicate emplacement modes. Flows with a normalized area closer to 1 are larger and those closer to 0 are smaller. Squares represent short pulse (10-s) and triangles represent long pulse (50-s). Flows in condition 2 are larger in area than those in condition 1 due to the increase in eruption duration and slight increase in erupted volume. Long pulse durations created notably larger area flows corresponding to higher normalized areas, especially at high Ψ values.

4.2.1. Flow propagation and emplacement modes

The symbols in Fig. 10 indicate the emplacement modes and pulse duration in relation to normalized area and flow depth. Note that these data are slightly different from those presented in Fig. 6, which counts all occurrences of emplacement mode regardless of whether or not it occurred in conjunction with other emplacement modes. Additionally, resurfacing was not considered a dominant process when occurring with other emplacement modes – and thus is not indicated on this and subsequent figures unless ≥20% of the flow surface was resurfaced when occurring with other emplacement modes. Flows displaying only resurfacing do not necessarily adhere to this threshold. Sheet flows, by

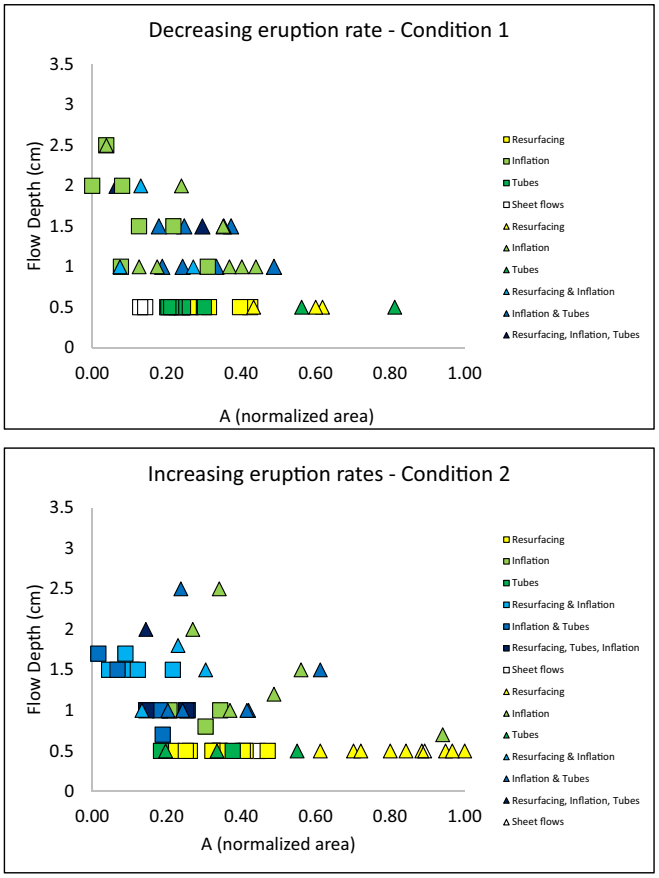

Fig. 10. The relationship between normalized area, flow depth, and the observed mode of emplacement. Flow depths and length scales do not significantly vary by condition. Flows displaying inflation (and other emplacement modes) tend to be thicker than other flows. Squares represent short pulse (10-s) and triangles represent long pulse (50-s). For flows displaying <20% areal resurfacing and other emplacement modes, resurfacing is not included as it is not considered a dominant emplacement mode in such a situation. Flows displaying inflation tend to be thicker and have smaller areas. Flows displaying singular emplacement modes tend to be thinner, with singular resurfacing present in flows of standard depth (~0.5 cm). Note that flows with multiple emplacement modes are more frequent in condition 2.

our definition, are not thicker than the nominal 0.5 cm, while flows displaying only tubes are not thickened throughout because tube formation is largely a localized process.

Flows dominated by only inflation are more common for decreasing eruption rates (condition 1) than for increasing eruption rates (condition 2). Flows with normalized areas <0.5 and depths >0.5 cm display inflation (typically in conjunction with other processes). Flows in condition 1 displaying only resurfacing or only tubes and even sheet flows have a range of normalized areas likely reflecting extruded wax volume differences between short and long pulses. In condition 1, sheet flows have normalized areas <0.2 while in condition 2, the two sheet flows observed have normalized areas of 0.34 and 0.89 likely reflective of the differences in extruded. Resurfacing is generally a localized process, typically occurring over <15% of the flow surface. However, at lower Ψ ($\Psi < \sim 8$) resurfacing can contribute more to flow thickening relative to higher Ψ ($\Psi > 41$) because resurfacing manifests as erupting lobes which can be thick and overlap. That said, resurfacing is nonetheless a localized process relative to inflation, which thickens the entire flow. No appreciable difference in flow depth is observed in condition 1 for the two different pulse durations, however, for condition 2 some flows with 50 s pulses have depths >1.7 cm.

Fig. 11 displays flow area versus time for both decreasing and increasing eruption conditions for a select number of experimental runs and provides information on flow propagation and can inform the timing of observed emplacement modes. Regardless of Ψ or eruption rate, all flows start out as simple, radial viscous gravity currents. At some point, however, the formation of a crust, decreasing flow rates at the flow front, and duration of the eruption stage, produce the onset of other emplacement modes. As expected, flows produced under decreasing eruption rates (condition 1) tended to grow at a slower rate during the pulse as the eruption rate decreased (flattening the curve). Conversely, flows erupted under increasing eruption rates (condition 2) tended grow at a faster rate (steepening the curve) as eruption rate increased. The data in Fig. 11a, displaying Ψ regimes for condition 1, are primarily defined by a region where inflation does not occur, which is at a combination of high Ψ and high Q. Widespread breakouts tend to occur at higher Ψ and higher Q. Other modes of emplacement do not have as clear of a pattern, occurring at a variety of different conditions. When inflation does occur, other emplacement modes tend to accompany it. In Fig. 11b, which displays experimental runs for condition 2, inflation is common. Widespread marginal breakouts also tend to occur in this grouping at higher Ψ and/or high Q. The data in Fig. 11 and video recordings of the selected experiments indicate that all of the experiments initially grow as radial sheet flows (viscous gravity currents), and other emplacement modes begin typically after half of the experiment duration has elapsed and especially during the pulse period (for decreasing eruption rates/condition 1).

Fig. 12 maps these dominant modes of emplacement in terms of mean eruption rate, mean Ψ, and pulse duration. Here we do not indicate the specific time when these emplacement modes might be occurring. Mean Ψ value takes into account the instantaneous Ψ and duration of each eruptive stage (i.e., the first stage and the second stage, or pulse). More than one mode of emplacement was observed in many of the flows (Fig. 12), with resurfacing again only considered a major process in conjunction with other emplacement modes when it repaved ≥20% of the flow surface. The data illustrate that inflation tends to dominate the left sector of the plot for condition 1, whereas resurfacing (when occurring alone) tends to dominate the right portion of the plot. This division indicates that endogenic thickening of the flow for condition 1 is dependent on Ψ and mean eruption rate. In flows with increasing eruption rates (condition 2), the division between resurfacing only flows and inflation dominated flows is similar to that in condition 1, although inflation is overall slightly more common in condition 2. This is because increasing flows favor inflation due to the longer duration of the initial lower flow rate that establishes a crust early in the experimental run. In general, in condition 2, crust formation exerts more control on emplacement mode than in condition 1 due to the longer durations of extrusion at low Q during the first stage of the eruption. In other words, crust exerts more control over emplacement mode when the flow initiates with a low flow rate and persists because a crust forms early in the process and then continues to control emplacement mode throughout the experiment.

Sheet flows are less common than inflation but more likely to occur under decreasing eruption rates (condition 1) and they tend to occur in the same field as inflation, however, they are primarily observed in flows with a 10 s pulse. For increasing eruption rates (condition 2), however, sheet flows occur in the same field as singular resurfacing and tubes albeit mostly – two out of three cases – for 10 s pulse flows. Flows with only tubes are rare and typically form at high mean eruption rates and intermediate-high Ψ for condition 1 and at high Ψ and low mean eruption rates for condition 2. However, when considered in conjunction with other emplacement modes tubes are present across all Ψ and Q for condition 1 and all Ψ and low-intermediate Q for condition 2.

Flows exhibiting multiple modes of emplacement (darker colors in Fig. 12), in other words the most complex flows, occur almost exclusively in the left sector for both conditions 1 and 2, corresponding to low-intermediate Ψ values. It should be noted that there is, however, more spread in condition 1, with some flows demonstrating multiple emplacement modes at high Ψ ($\Psi > 41$). Additionally, experiments in condition 1 with multiple emplacement modes are exclusively at 50 s pulse durations. In contrast, flows with multiple emplacement modes in condition 2 are more tightly clustered at low-intermediate Ψ ($\Psi < 21$). The appearance of inflation at conditions that favor crust preservation is the main cause for this distinction.

4.3. Summary of findings for decreasing (condition 1) and increasing (condition 2) eruption rates

- Increasing eruption rates (condition 2) favor resurfacing over inflation perhaps related to greater extruded volumes. However, inflation is more common for flows with increasing eruption rates and more dependent on Ψ than for flows with decreasing eruption rates (condition 1). This effect is likely tied to the longer duration of low-Q extrusion during the initial stage of the eruption for condition 2 and corresponding establishment of a strong yet pliable crust.
- Resurfacing as a singular emplacement mode is favored at intermediate to high Ψ ($\Psi > 41$) for both conditions.
- Marginal breakouts were the 2nd most common mode of emplacement in condition 1 and the most common mode of emplacement for condition 2.
- Marginal breakouts are almost always localized under decreasing eruption rates (condition 1) and occur primarily under long pulse durations. Under increasing eruption rates (condition 2), localized marginal breakouts occur for short pulse durations, while widespread marginal breakouts occur under long pulse duration. In flows with increasing eruption rates, high Ψ values ($\Psi > 41$) favor widespread breakouts, whereas low Ψ ($\Psi < 8$) values favor localized breakouts.
- Inflation tends to occur more readily at low Ψ ($\Psi < 8$) values for both increasing (condition 2) and decreasing (condition 1) eruption rates, although inflation is also observed at low mean eruption rates for high Ψ ($\Psi > 41$) in decreasing flow conditions. For decreasing eruption rates, inflation is more likely to occur under long pulse conditions, whereas there is no dependence on pulse duration for increasing eruption rates.
- Tube formation is rarer than other emplacement modes, but are most likely for 50 s pulse durations under decreasing eruption rates (condition 1). Tubes are equally likely to occur at 10 s and 50 s pulse durations for increasing eruption rates (condition 2). In addition, when occurring with other emplacement modes, tubes do not have a significant pattern with mean effusion rate or Ψ.

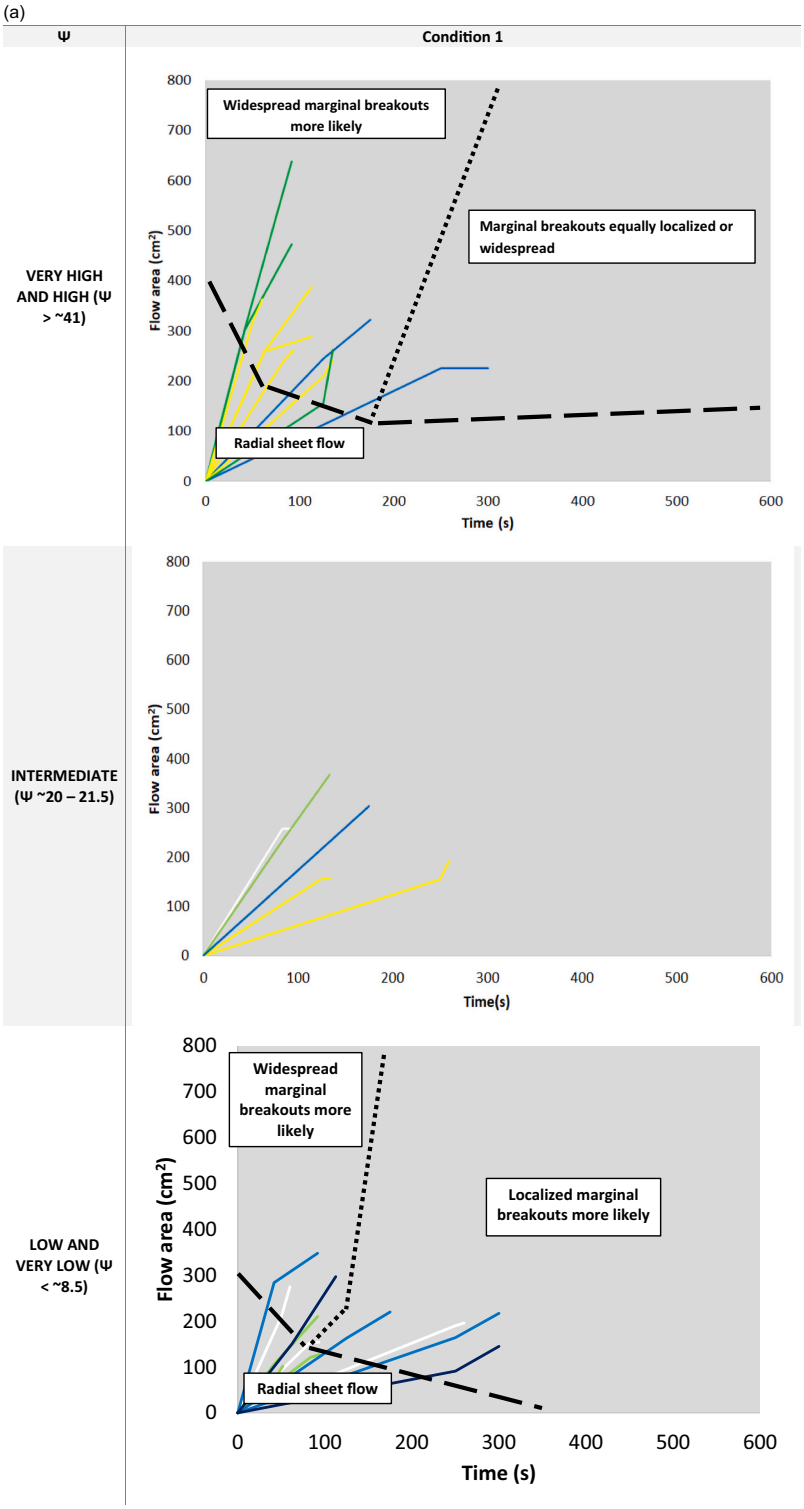

Fig. 11. Select data from flows erupted under the range of Ψ conditions for conditions 1 and 2 are presented here with flow area as a function of time. Curves have been color coded by emplacement mode using the same scheme in Figs. 9 and 10. With yellow, light green, green, light blue, blue, dark blue, and white representing resurfacing; inflation; tubes; resurfacing and inflation; inflation and tubes; resurfacing, inflation, and tubes; and sheet flows, respectively. Flatter curves with longer durations are generally associated with lower mean eruption rate values. Dashed lines do not represent hard boundaries, but general regimes were observed emplacement modes likely occur. Intermediate Ψ plots have been left intentionally blank as the observations at high and low Ψ represent end members. (**a**) Select flows observed in condition 1 at decreasing and eruption rates for high to low Ψ for short (10 s) and long (50 s) pulse durations. The flows are mainly separated by when inflation is observed. (**b**) Select flows observed in condition 2 at increasing eruption rates for high to low Ψ for short and long pulse durations. The flows are mainly separated by when tubes and different types of marginal breakouts occur. (For interpretation of the references to color in this figure legend, the reader is referred to the web version of this article.)

(b)

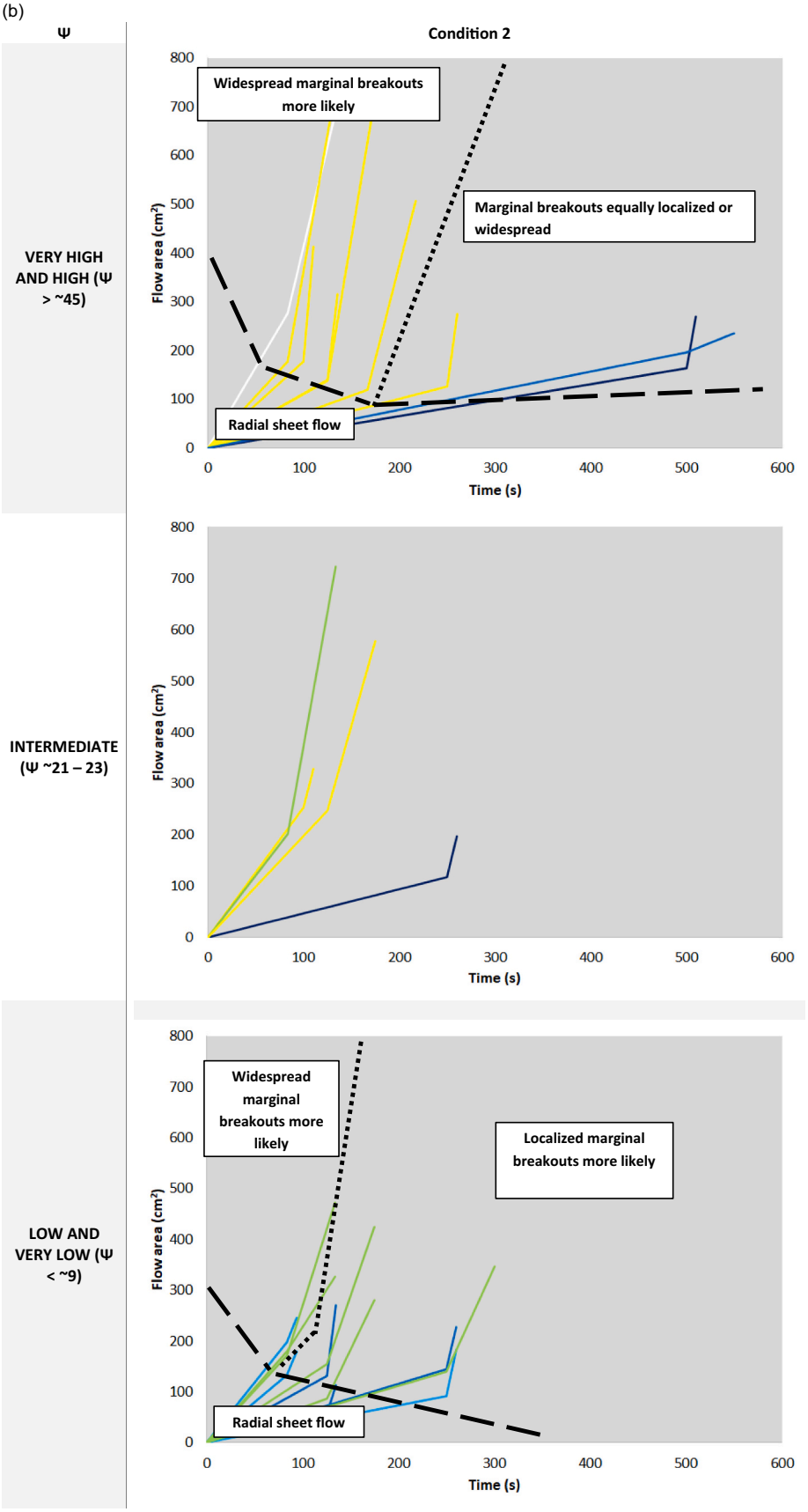

Fig. 11. (*continued*).

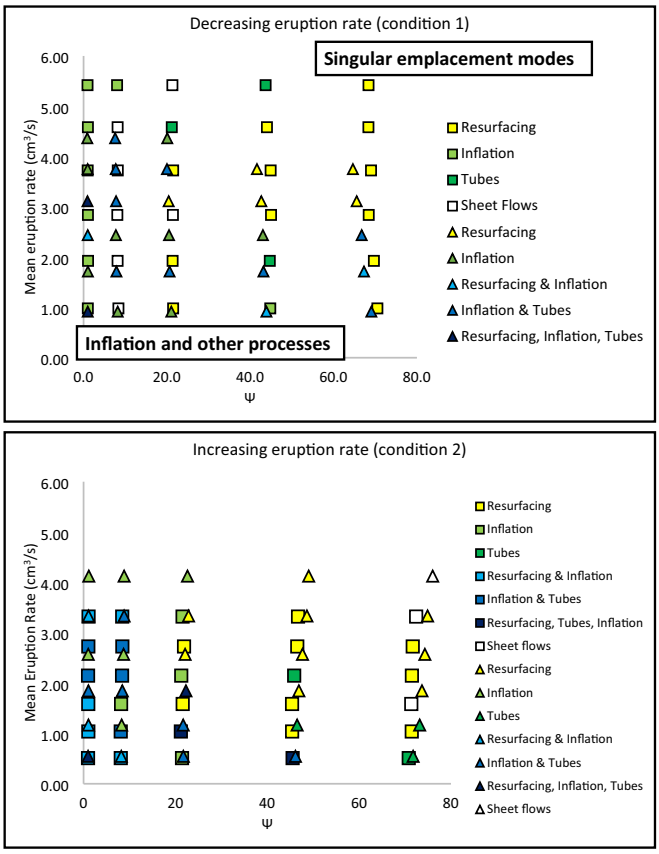

Fig. 12. The distribution of dominant emplacement mode with respect to mean Ψ and mean eruption rate. Squares represent short pulse (10-s) and triangles represent long pulse (50-s). Offset between squares and triangles reflect an artifact of experimental design (i.e., mean eruption rates and mean Ψ due to differences in duration of eruption). A divide – highlighted by the transition from lighter to darker colors – between flows with singular modes of emplacement and those with inflation and other modes is evident in both conditions. Marginal breakouts are not depicted, although they occur primarily at intermediate-high Ψ for condition 1 and for every flow in condition 2. For condition 1, resurfacing and tubes as singular emplacement processes occur primarily at higher Ψ and/or higher mean eruption rate. Simple sheet flows and inflation (with other modes of emplacement) occur primarily at low to intermediate Ψ and/or low to intermediate mean eruption rates. For condition 2, flows with singular resurfacing and tubes and sheet flows occur primarily at intermediate-high Ψ. Inflation is at low-intermediate Ψ. As in condition 1, flows in condition 2 with inflation (and other emplacement modes) also tend to cluster near the left of the plot at low-intermediate Ψ.

- When emplacement mode is indicated on the mean eruption rate vs mean Ψ-*value* plot, a regime diagram of emplacement modes is produced. With decreasing eruption rates, resurfacing is favored to the right of the space, whereas pure inflation or complex flows featuring some components of inflation are favored on the left portion of the plot. For increasing eruption rates, the division between resurfacing and inflation is similar: pure resurfacing, tubes, and sheet flows occur at higher Ψ ($\Psi > 41$) while complex flows with inflation occur at low-intermediate Ψ ($\Psi < 21$).

5. Discussion and implications

As noted in the qualitative descriptions, video recordings of the experiments and data in Fig. 11 support the notion that the investigated emplacement modes occur after the flow has matured to a certain degree. Typically, the emplacement modes of interest were not observed until over halfway through the eruption, with many initiating during the period of decreasing or increasing eruption rate (the pulse). The bends in the curves may reflect a combination of decreasing or increasing forward propagation of the flow front (via decreasing or increasing flow rate at the flow front), resurfacing (thickening vs areal increase), marginal breakouts (advance of the flow front), and/or inflation (as mass is diverted to thickening the flow instead of increasing its area).

These data suggest that factors other than localized flow rate contribute to the slowing of flow advancement and increase in flow area. For higher Ψ ($\Psi > 41$), the propagation curves are primarily separated by whether or not inflation occurs. Inflation is more likely at lower eruption rates, and when inflation occurs, it tends to occur in the presence of other emplacement modes. For lower Ψ ($\Psi < 8$), the propagation curves are separated primarily by when tubes – and to a lesser extent – resurfacing occurs. The propagation rates provide an understanding of how the flow propagates with time and illustrate the impact of changing the eruption rate during the pulse (i.e., shallowing or steepening of the curve). All flows begin as simple viscous gravity currents (i.e., simple sheet flows as defined here). Emplacement modes tend to occur after more than half of the eruption duration has lapsed.

An important factor to consider when interpreting our results are the variables that go into Ψ. Ψ is a function of effusion rate, temperature, and time. Although it describes the crust conditions and we sometimes

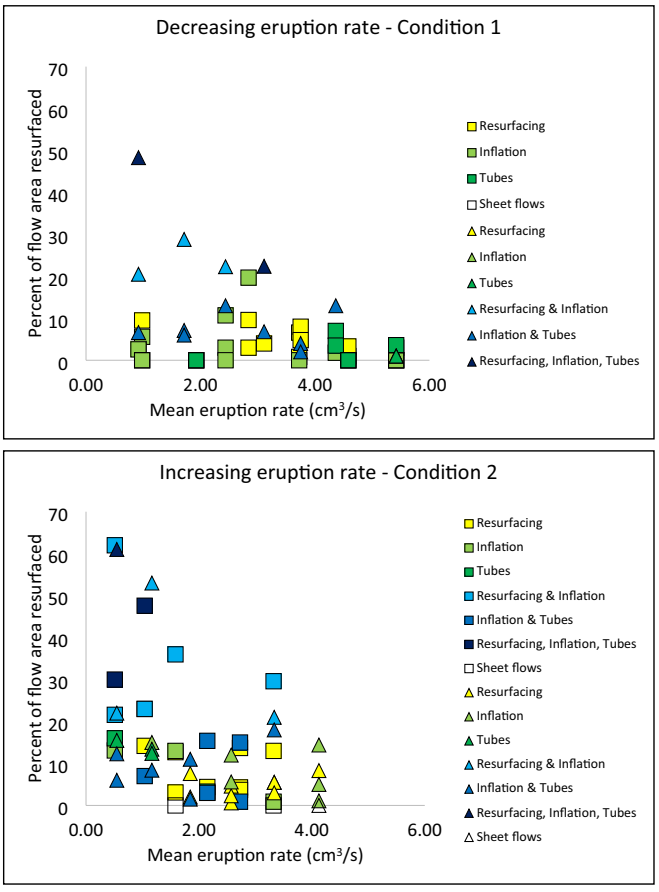

Fig. 13. The percent of flow area resurfaced for a given mean eruption rate with respect to emplacement mode. Squares represent short pulse (10-s) and triangles represent long pulse (50-s). Horizontal offset of squares and triangles is an artifact of experimental design. A relationship exists between the mean eruption rate and the percent of flow area resurfaced during an eruptive event. The extent of resurfacing decreases with increasing mean eruption rate for flows displaying inflation and other modes of emplacement. While the relationship exists in both conditions, it is more pronounced in condition 2. For all other flows, there is no strong correlation between mean eruption rate and % of flow area resurfaced. R = resurfacing; I = inflation; T = tubes.

treat the two variables (eruption rate and Ψ) as separate, there is a flow rate component built into Ψ indicating the rate at which heat is advected by the flow. Hence, high Ψ (Ψ > 41) flows will flow faster than the time it takes for diffusion to produce a surface crust. Using mean Ψ for a given experimental run takes into account how changes in the effusion rate impact Ψ although the difference is not large. For a given high Ψ experiment in condition 1 with an instantaneous eruption rate of 6 cm^3 erupted at 26.7 °C, Ψ is approximately 45. During a pulse at half the initial eruption rate (3 cm^3), instantaneous Ψ drops to approximately 37. The mean Ψ for this experiment would be 43.7 (for the short pulse) and 41.2 (for the long pulse). Thus, changing the effusion rate has a noticeable impact on the Ψ value, although it doesn't change the Ψ regime which in this case would be considered 'high' and expected to produce levees and a weaker surface crust. This is significant when considering that an average Ψ might be more practical when characterizing lava flows or lava flows fields wherein a dominant morphology is observed but variable eruption conditions cannot be discounted.

5.1. Modes of emplacement

5.1.1. Resurfacing

Resurfacing – essentially *intraflow* surface breakouts – is commonly observed on active flows, specifically pāhoehoe flow fields. Resurfacing differs from breakouts at the flow margin, because the breakout emplaces a new lobe onto the surface of the flow itself and it can occur at any location proximal or distal to the flow source. Breakouts at any location in lava flows generally occur when an insulating crust ruptures, which could be due to overpressurization induced by an increase in flow rate or continued inward solidification of the flow crust [e.g., Hoblitt et al., 2012].

In our study, resurfacing was observed in the majority of experiments for every condition regardless of mean eruption rate, pulse duration, or whether the eruption rate decreased or increased. Resurfacing has a dependence on Ψ for decreasing eruption rates (condition 1), with a higher occurrence at intermediate to high Ψ (Ψ > 21) but is limited in spatial extent. The resurfacing in these flows occurs either toward the end of the initial stage of the eruption or during the pulse such that the wax takes advantage of any weak points in newly formed crust. For increasing eruption rates (condition 2), resurfacing is greater in areal extent and occurred primarily during the pulse when the eruption rate was higher. It is important to note that once resurfacing created a pathway through the surface crust it was not uncommon for subsequently erupted wax to continue to take advantage of this pathway at any point after its creation.

Resurfacing was frequently observed and commonly occurred in concert with other emplacement modes. Based on our results resurfacing is much more likely when there is a sudden increase in eruption rate, however, in general, the volume of the wax devoted to resurfacing is very small. Far more wax is mobilized in inflation and marginal breakouts (see below) than in resurfacing. For that reason, resurfacing did not contribute much to flow thickness, except at low / very low Ψ when it occurred mostly as overlapping bulbous lobes. Instead, flow thickness increases primarily when the flow is initially emplaced or when it is inflated. Some of the conditions that favor resurfacing (such as a sudden increase in flow rate) also favor increasing spreading rates, although the resurfacing itself does not contribute to the increase in spreading rate, but is instead a side effect of an increased spreading rate that may indirectly cause crust ruptures. In experimental runs with a larger degree of resurfacing, sometimes the wax flowed past the flow margin and increased the size of the flow, typically at low to intermediate Ψ values.

The frequency of resurfacing was found to be dependent on Ψ only for decreasing eruption rates (condition 1). Flows displaying only resurfacing were also dependent on Ψ (Fig. 12). In condition 1, resurfacing was less likely at low and very low Ψ. At short pulses (10 s), there was an observed decrease in resurfacing for intermediate Ψ, however at long pulses (50 s) this was not observed suggesting that the longer pulse length allowed for conditions more favorable to resurfacing. This observation suggests that the formation of a coherent, insulating, and immobile crust produced at lower Ψ prevented wax from escaping to the surface. The decreased eruption rate in condition 1 also reduced the pressure under the crust which may have also precluded resurfacing in some cases. However, the slight increase in frequency of resurfacing for experimental runs with a long pulse suggest that if given enough time, the molten wax is able to fracture the crust and resurface the flow.

The frequency of resurfacing shows no dependence on Ψ for increasing eruption rates (condition 2), however flows displaying only resurfacing are dependent on Ψ (Fig. 12). Furthermore, flows displaying only resurfacing show no dependence on eruption rate. Thus, a sudden increase in the eruption rate at a volcanic vent may increase the likelihood of surface breakouts on an active lava flow regardless of the Ψ of the eruption.

Although resurfacing appears to be a common process, we must also consider the extent of resurfacing – that is, what percentage of the flow surface is resurfaced during these events. For decreasing eruption rates (condition 1), the vast majority of instances of resurfacing effected <10% of the flow area. At lower mean eruption rates for condition 1, the areal extent of resurfacing increased for some flows displaying multiple emplacement modes (Fig. 13). For increasing eruption rates (condition 2), the vast majority of flows that experienced resurfacing had <15% of the flow area resurfaced, representing an increase in the average degree of resurfacing overall relative to condition 1. A dependence on Ψ and Q was observed for condition 2 at lower Ψ regimes (Fig. 14), with half of the flows in low Ψ regimes having resurfacing percentages 13–30%, and those at very low Ψ, ~20–60% although this occurs exclusively for flows displaying multiple emplacement modes. Likewise, the highest resurfacing percentages were observed at mean eruption rates <1.5 cm^3/s. At lower Ψ values, it is important to note that the resurfacing takes on a different manifestation with the flow becoming more conducive to the stacking of overlapping bulbous lobes of extruded wax. Therefore, although resurfacing is frequent it is not necessarily the dominant emplacement mode in a given flow.

These interpretations are not surprising if we consider flow environments observed in nature which are analogous to those in the lab. Higher Ψ regimes in nature tend to manifest as channelized lava flows and perhaps exotic sheet flows observed on other planets. In those conditions, we would expect resurfacing to be minimal – in the case of a lava channel it could manifest as lava lapping onto levees or repaving portions of the flow near the terminus (which would be considered a low Ψ environment). Low Ψ regimes are more synonymous with pāhoehoe flow fields. Breakouts are common in pāhoehoe fields as lobes expand, rupture, and repave or advance the flow. The continuum of Ψ morphologies also means that a single lava flow undergoes different flow and crustal conditions over its entire length. Therefore, these emplacement modes may occur at different rates over the length of the flow.

5.1.2. Marginal breakouts

Marginal breakouts occurred in most experiments, although they were less likely to occur under decreasing flow rates (condition 1), where the crust at the flow margins solidified and prevented continued flow propagation. The number of marginal breakouts and whether or not the breakouts were circumferential (mobilization of >50% of the flow front), localized, or circum-local (some combination of both) depended on Ψ and pulse duration in condition 1. The longer pulse duration allowed more time for wax to flow beneath the crust and emerge at the flow front. In most cases these breakouts were localized, meaning most of the flow front was not active at any given time. The implications are that decreasing eruption rates are more likely to produce a few significant breakouts instead of many, smaller breakouts. Circum-local breakouts – those in the 'both' category that resulted in ~50% of the flow margin experiencing breakouts (Fig. 6) – were most common at the lowest Ψ values which has implications for pāhoehoe fields for which this Ψ regime is analogous. These observations suggest that even at

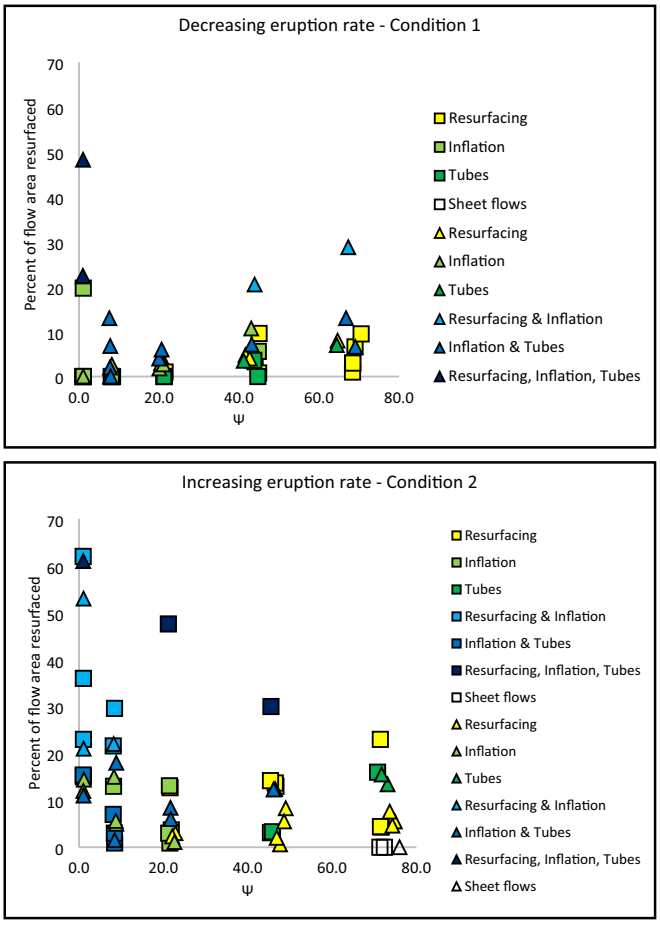

Fig. 14. The percent of flow area resurfaced and mean Ψ with respect to emplacement mode. Squares represent short pulse (10-s) and triangles represent long pulse (50-s). Horizontal offset of squares and triangles is an artifact of experimental design. For condition 1, some flows with inflation and other modes display higher degrees of resurfacing at lower ($\Psi < 21$) and higher Ψ ($\Psi > 41$), but most flows have no correlation with % of area resurfaced and Ψ. For condition 2, flows with inflation and other modes present have decreasing % of areas resurfaced with increasing Ψ. Other flows are unaffected by this trend. The lower extent of resurfacing at increasing Ψ is likely due to a more tenuous surface crust and the disruption of said crust during the pulse. R = resurfacing; I = inflation; T = tubes.

decreasing eruption rates, a portion of the flow front could remain active in the form of limited, localized marginal breakouts.

Marginal breakouts occurred in every experimental run for increasing eruption rates (condition 2) except one. The likelihood of marginal breakouts in this condition had no observed relationship with pulse duration given the parameters we controlled for, however, whether or not the breakouts were widespread or localized depended on Ψ. The stronger crust present at lower Ψ regimes prevented widespread breakouts at the flow margin and instead favored eruptions of wax at discrete locations at the flow front. These localized breakouts, however, can be just as voluminous and impactful to flow advancement as widespread mobilization of the flow front. Pulse duration did play a role in the extent of marginal breakouts. Widespread marginal breakouts occurred almost exclusively for long pulses (50 s), with the effect being greatest for low and very low Ψ. Given a long enough pulse at higher eruption rates, the strength of the wax could be overcome and activity at the flow front increased.

5.1.3. Inflation

Inflation of lava flows is thought to be a primary way that many non-channelized lava flows achieve deposit thicknesses of meters to tens of meters, especially in large igneous provinces such as the Deccan Traps and Columbia River Basalts, although inflation has also been observed in silicic flows [e.g., Hon et al., 1994; Self et al., 1996; Sheth, 2006; Tuffen et al., 2013; Rader et al., 2017; Carr et al., 2019]. Complimenting and expanding the design used by Rader et al. [2017], our experiments investigated how unsteady eruption rates impact inflation. Inflation requires a coherent, insulating crust. A lower effusion rate, while amenable, may not be strictly required. In nature, inflation can occur in pāhoehoe flow fields with relatively low effusion rates due to interconnected pockets of melt [Hon et al., 1994]. However, those flow rates can increase gradually or spike due to changes of the vent flux or local flow conditions.

In our experiments, inflation occurred whether or not the eruption rate increased (condition 2) or decreased (condition 1), as long as the crust was strong enough to contain the majority of the still molten wax. In other words, inflation is strongly dependent on Ψ. For both conditions, inflation is more frequent in lower Ψ – with inflation rarely occurring at higher Ψ. This finding is supported by condition 1 and 2 data. Inflation is rare under decreasing eruption rates for the short pulse experimental runs because there was insufficient time for a coherent crust to form and a detectible volume of wax to accumulate beneath it. For long pulse experimental runs in condition 1, inflation is more frequently observed. Under increasing eruption rates, the frequency of inflation is the same for 10 and 50-s experimental runs indicating that the lower initial eruption rates allowed a coherent, insulating crust to form, thus promoting conditions favorable to inflation during the later high-Q pulse. However, in many instances a dramatic increase in the eruption rate (condition 2) led to rupturing of the solid wax diverting mass from inflation into resurfacing events and marginal breakouts. Higher Ψ values describe regimes where the timescale of crust formation is long and horizontal propagation of the flow is fast. Thus, these are conditions that do not favor the formation of a coherent, insulating crust.

An important distinction between conditions 1 and 2 is *when* inflation occurs. For decreasing eruption rates, inflation was observed once the flow rate decreases during the pulse. For increasing eruption rates, inflation was observed during both the initial stage of the eruption when flow rates are low and a crust can form allowing the flow to inflate and/or during the final stage of the eruption after a competent crust has formed or after a resurfacing or marginal breakout event.

Inflation commonly thickened flows by 2–3× their non-inflated counterparts, with some flows inflating even more (Fig. 5, very low Ψ panels). The final thickness of the flows was correlated with Ψ regime, with thicker flows observed at lower Ψ. This reflects the readiness for flows in low and very low Ψ regimes to produce and maintain a competent, insulating yet flexible crust. Inflated flows tended to be smaller in area as spreading rates at the margin were lower due in part to the storage of wax beneath the crust (images and more detailed description of inflated wax flows can be found in Rader et al., 2017). Inflation frequently occurred in the presence of resurfacing and other emplacement modes. This is most evident at very low Ψ, where flows analogous to pāhoehoe or pillow lavas would inflate and the flow would advance via bulbous lobes. Resurfacing often took the form of overlapping bulbous extrusions that erupted on the flow surface. The storage of wax underneath the crust made resurfacing in the form of bulbous extrusions on the flow surface more likely than marginal breakouts. Overall, these observations are consistent with the conditions in which inflation is observed in real lava flows.

5.1.4. Tubes

The tubes produced in our wax flows most closely approximate the morphology and formation process of tubes formed in pāhoehoe flows with fluid interiors due to the lack of slope in the experimental set up. Tubes produced via roofing over of open channels did not occur in our experiments. The rarity of tubes likely lies in the conditions needed to

produce tubes: steady effusion rates, low effusion rates, the formation of a roof of crust, and generally longer eruption durations [e.g., Greeley, *1972*; Malin, 1980; Calvari et al., 2002]. By the nature of our experimental design, the effusion rate was not constant during the duration of the run and pulse durations were relatively short. The frequency of tubes was higher in decreasing flows (condition 1) for the long pulse (50-s) because there was more time for the flow to reach steady conditions at a lower eruption rate. Tubes were even more likely to form in increasing flows (condition 2) for both 10- and 50-s pulses since initial eruption rates were half that of the initial value for condition 1. Similar observations were noted during the 1999 summit eruption of Mt. Etna, where long periods – weeks to months – of relatively steady effusion rates promoted lava tube formation [Calvari et al., 2002]. In contrast, rapid fluctuations in the effusion rate suppressed tube formation and promoted shorter, volume-limited flows [Calvari et al., 2002]. In general, the lower occurrence of tubes relative to other emplacement modes in our experiments could suggest that the added instability of the eruption, or unsteadiness, discourages tube formation and perhaps promotes different emplacement modes. This assessment would be congruent with the conditions in nature necessary for lava tube formation.

The occurrence of tubes had no dependence on mean eruption rate or Ψ for conditions 1 and 2. However, flows displaying only tubes occurred primarily at high mean eruption rates (> 4 cm^3/s) and high Ψ ($\Psi > 41$) for condition 1 and low mean eruption rates (<2 cm^3/s) and high Ψ ($\Psi > 45$) for condition 2. This observation suggests that – at least in our experiments – a low eruption rate is not necessary to initiate tube formation. Instead, the conditions necessary to produce a competent overlying crust and steady eruption and flow rates may be more important to promoting tube development beneath said crust. In decreasing flows (condition 1), those tubes formed after the crust had solidified and when eruption rates decreased. In increasing flows (condition 2), tubes initiated during the first stage of the eruption when flow rates were low, and then when flow rates increased, the tubes were already formed and seemed to persist. Regardless of condition, the frequency of tube production was rare compared to the frequency of inflation or resurfacing. Tubes did not appear to be correlated with flow depth. They were observed in flows that had experienced no thickening as well as flows that were thickened by resurfacing and/or inflation. These correlations suggest that the conditions favorable to tubes were sometimes also favorable for resurfacing and/or inflation.

5.2. Erupted volumes – sheet flows, singular emplacement modes, and short duration pulses

The total erupted volume for a given experimental run was a function of the initial 250 cm^3 erupted and the volume of wax erupted during the pulse (either 10 or 50-s). The total volume of the pulse ranged from 5 to 300 cm^3. For short pulse duration experiments at lower eruption rates, this means that a smaller volume (5–30 cm^3) of wax was erupted than for short pulse duration experiments with higher eruption rates (20–60 cm^3) let alone those with long pulses (25–300 cm^3). This volumetric difference was particularly noticeable for flows erupted in condition 1 with short pulses, which erupted only 5–30 cm^3 of wax. Those flows that experienced the smallest volumes of erupted material during the pulse had simpler morphologies and typically singular emplacement modes (e.g., resurfacing only or tubes only). For condition 1 (instantaneous decrease in eruption rate), most sheet flows – those flows only radial flow – were observed at low and intermediate Ψ (8–8.4; 21.3–21.4) and in flows with short pulses. This suggest that not enough wax was erupted under these conditions to impact flow propagation. One way to interpret this is that short duration changes in the flow rate of a lava flow with low flow rate and a stable crust will likely not be recorded in the rock record. Conversely, with respect to sheet flows observed in this study, the three sheet flows observed in condition 2 occurred at very high Ψ ($\Psi > 71.4$) and 2 out of 3 of those in runs with short pulses. Although greater than that erupted during condition 1, the volume of wax for the 2 short pulse sheet flows was minimal (30 and 60 cm^3) and erupted under conditions with a tenuous surface crust. The dearth of sheet flows produced in condition 2 suggests that a different mechanism is at work than for condition 1, perhaps related to either the ability of a surface crust to establish itself at lower eruption rates or the ability of an instantaneous increase in eruption rate to produce resurfacing, marginal breakouts, and/or inflation.

5.3. Reproducibility of results

While a variety of studies have demonstrated the reproducibility of Ψ morphologies in the laboratory, in this study, we have investigated four different emplacement modes under unsteady conditions at the vent which result in more complicated flow morphologies. Even if one were to attempt to reproduce a given experimental run using the correct wax and water temperature, eruption rate, Ψ, and pulse duration, there is no guarantee that the exact set of processes would occur for a given flow. For example, in cases with the same flow conditions except pulse duration, flows with 10 s pulses displayed simpler morphologies than those with 50 s pulses. The 10 s pulse experiments therefore usually had smaller flow areas, less resurfacing, and/or limited or no marginal breakouts. Moreover, what makes the study of lava flows difficult is the complex physics and phenomenology that drives flow propagation. Our results are based on a large number of experiments ($n = 120$) with overlapping experimental conditions, and they therefore demonstrate what emplacement modes and flow conditions are more likely for given regimes. A flow produced under decreasing flow rate conditions with low to intermediate mean eruption rates and low to intermediate Ψ will likely exhibit an extensive, competent crust and will be susceptible to localized marginal breakouts, inflation, and tubes. In the case of increasing flow rates, said flow would likely exhibit more extensive resurfacing and a higher likelihood of widespread activation of the flow front. The inclusion of dimensionless parameters, such as Ψ and normalized area, make it possible to compare regimes in future work.

5.4. Comparison with simple lava flow: early stage of Fagradalsfjall eruption, Iceland

We were able to make observations of effusion rate affecting emplacement mode during the earliest stages of the *Fagradalsfjall* eruption, which was live streamed by RÚV and put on Youtube in a timelapse format (e.g., https://www.youtube.com/watch?v=PLJeUMzlzZw; RUV 2021). Footage begins at 11:07 on March 20th, 2021, with lava flowing from the vent in three locations (Fig. 15). Most of the lava visible to the camera flows into a standing pond to the left side of the vent. There are several small cascades over the banks of the pool, two or three of which feed longer channels. The majority of the lava is being emplaced via resurfacing or as resurfacing flow extending past the edge of the solidified flow. Because this footage is from such an early stage in the eruption, we can link changes of the local effusion rate at the vent to the emplacement mechanism. Below is a description of how a decrease in effusion rate resulted in the formation of a tube, which activated and produced a marginal breakout after a subsequent increase in effusion rate.

11:45 - The far right opening of the vent has a ***large obstruction of spatter*** that has accumulated at the lip of the cone (Fig. 15a).

12:02 – spatter wall collapses into the vent, followed by a vigorous series of explosions and ***increased flow*** from the vent (Fig. 15b). The increased effusion rate builds a ***new channel*** reaching the edge of the flow on the right side of the screen.

14:30 - This new flow expands the footprint of the eruption and forms the preferred pathway for a channel that eventually crusts over as ***effusion rate decreases*** (Fig. 15c).

15:20 - Vent begins to accumulate another spatter obstruction. The left branch of this channel ***crusts over forming a tube*** (Fig. 15d). As the flow rate remains steady for the next hour, the flow extends its footprint

via the right branch of the channel.

16:31 - Accumulation of spatter at the vent collapses again resulting in another ***increase in local effusion*** rate from the vent (Fig. 15e).

~16:40 - A confounding factor, the right branch of the channel reaches the creek. The advancement of the flow front stalls possibly because of the water interaction, pressurizing the lava up channel.

16:43 and 16:46 - a series of pulses of lava from the vent follow ***increasing the local effusion*** rate in the upper channel.

16:49 – Upper channel overflows.

17:32 – ***Marginal breakout*** from tube-fed flow begins (Fig. 15f). This tube continues to feed the flow front for another 3 h.

During the 9 h of this infant eruption, we observed the following relationship between effusion rate and emplacement mechanism. An increase in effusion rate resulted in resurfacing and channel formation. A decrease in effusion rate resulted in channel crusts over and forms a tube. A subsequent increase in effusion rate caused a marginal breakout from a tube. While some differences exist, this reflects the common mechanisms found in our experiments (i.e., tube formation most frequent in periods with minimal crust disruption, marginal breakouts and resurfacing most frequent in experiments with increasing effusion rates), suggesting wax experiments reasonably describe the relationship between local effusion rate and flow emplacement mode. The detailed ways in which the experiments deviate from the real-world eruption (e.g., tube formation inhibited in experiments) can be attributed to differences in complexities, for example, the experiments were not conducted on a slope.

Our description of the Fagradalsfjall eruption was only one short period when the flow was relatively simple, so these results should not be universally applied to all eruptions. Similarly, the local effusion rate was very dependent on what other avenues the lava flow traversed. However, our observations of this flow help to demonstrate the utility of the wax experiments when conditions can be carefully controlled for.

5.5. *Hazards applications and modelling implications*

Modelling lava flows remains challenging due to the multiphase nature of the fluid, solidification and crust formation, and the resultant complex phenomenology of the flows. As a result, there is a limited number of physics-based models that simulate important processes and conditions that occur in lava flows, which include crystallization, and degassing [e.g., Pinkerton, 1987; Dietterich et al., 2017]. The incorporation of complex phenomenology of lava flows would improve model application to hazards mapping. As stated in the introduction, many models (both inundation and propagation based) predict a flow's likely

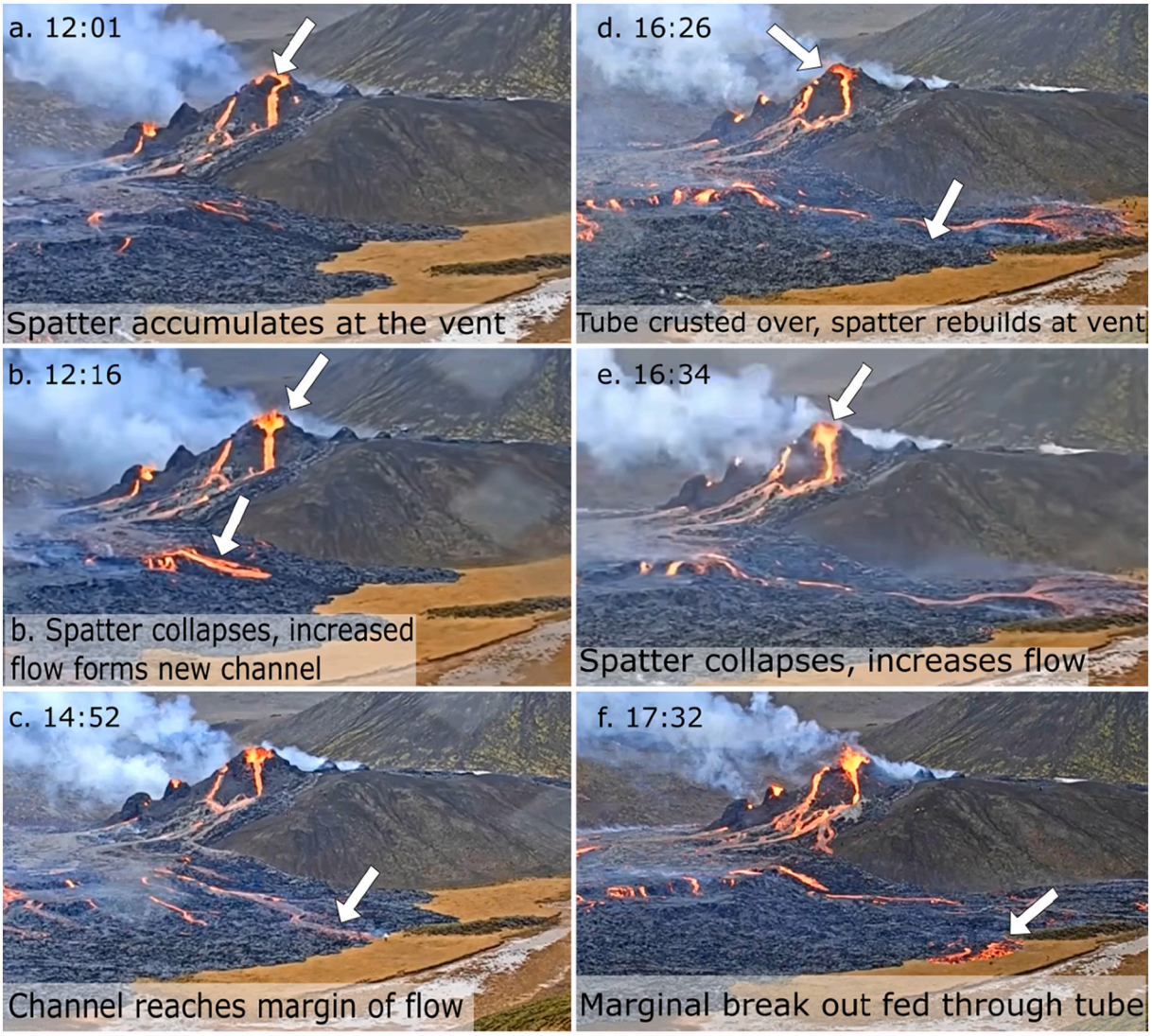

Fig. 15. Screen grabs of the live stream of the 2021 eruption in Fagradalsfjall, Iceland on March 20th. These relationships were only able to be seen because this was the beginning of the eruption and more complicated networks of flow pathways were not yet established.

path based on a few key parameters – typically underlying slope or effusion rate [e.g., Vicari et al., 2007; D'Michieli Vitturi and Tarquini, *2018*]. While inundation models can do a reasonable job of reproducing historical flows and provide a beneficial first-order analysis, they were not designed to simulate the complexities associated with lava flow propagation, such as different emplacement modes. Propagation models such as FLOWGO or MAGFLOW, on the other hand, can account for simplified crustal effects and are an improvement upon crust-free inundation models. That said, these propagation models are not necessarily intended to predict the evolution of complex morphologies that readily occur in the lab and field. Laboratory experiments, while still not as complex as real lava flows, can reveal the conditions under which different modes of emplacement are favored, and can therefore be used in conjunction with numerical models to adapt them to account for greater complexity.

For example, in the probabilistic model MrLavaLoba, slope is the primary variable that affects where the next parcel of lava will flow. It models the lava flow's progression as a series of elliptical lobes and is aimed at determining the most likely zone of inundation by a given lava flow [D'Michieli Vitturi and Tarquini, *2018*, https://github.com/demichie/MrLavaLoba]. In addition, MrLavaLoba uses a lobe exponent, ranging from 0 to 1, to describe the likelihood of the most recently emplaced lobe to become the parent of the next lobe to form. A lobe exponent value of 0 indicates that the youngest lobe will produce the next lobe, resulting, over time, in a chain of singular lobes. A value of 1 would give equal probability to any lobe producing a new lobe and results in wider, stacked, more complex flows. Therefore, a lobe exponent of 0.5 would imply an equal likelihood of the youngest lobe or any other lobe producing the next lobe. This exponent is currently a free parameter in the code, and is calibrated to some extent on past lava flows from a particular vent. Our experiments offer an opportunity to choose the exponent based on physical characteristics of the eruption – Ψ and effusion rate, or Q. For increasing flow rates (condition 2), a lobe exponent < 0.5 takes into account the widespread marginal breakouts. For decreasing flow rates (condition 1), a lobe exponent of >0.5 accounts for the localization of marginal breakouts. Resurfacing and inflation would be modeled here as "stacking". The likelihood of resurfacing or inflation occurring in a given flow increases as the lobe exponent approaches 1.

The following generalizations can be made: 1) significant stacking (inflation or resurfacing) should be most common at a combination of lower Ψ and lower effusion rates; 2) discrete lobes at one or two locations (localized breakouts) at the flow front should be most common at decreasing eruption rates, short periods of increasing eruption rates, and low-intermediate Ψ ($\Psi \leq 21$) for increasing eruption rates; and 3) widespread breakouts (propagation) along most of the flow front should be favored during increasing eruption rates, especially at longer intervals of increased rates, and predominantly intermediate-high Ψ ($\Psi \geq 21$). On the other hand, low-intermediate Ψ ($\Psi \leq 21$) and a well-developed, insulating crust – regardless of effusion rate – favor inflation, which is not accounted for in this lava flow model.

6. Conclusions

We have demonstrated that the tempo of an eruption – increasing and/or decreasing the eruption rate for a period of time – has implications for the formation and preservation of lava flow emplacement modes, specifically resurfacing, marginal breakouts, inflation, and tube formation. This study provides valuable insight into lava flow dynamics and constraints for probabilistic and physics-based models which seek to replicate existing lava flows and forecast future ones. The conclusions of this study are as follows:

1. The formation and sustainability of a coherent, insulating crust determines whether or not resurfacing, marginal breakouts, inflation, and tube formation will occur, which fundamentally determines how the lava flow distributes its volume during emplacement (on surfaces with minimal slope).
2. Increasing eruption rates (condition 2) at the vent disrupt the crust promoting marginal breakouts, resurfacing, and sheet flows during the pulse. However, the stronger the crust, the less disruptive increasing eruption rates will be and modes of emplacement such as inflation could occur.
3. Decreasing eruption rates (condition 1) preserve the crust and allow for the crust to spread and thicken. These conditions can favor localized marginal breakouts, inflation, and tube formation as the wax beneath the crust forms discrete pathways while propagating to the flow front. However, at high mean eruption rates, resurfacing may occur albeit with a tendency to occur at higher Ψ ($\Psi > 41$) values.
4. Resurfacing occurs under both decreasing and increasing eruption conditions, although it is more frequent under increasing conditions. Resurfacing occurs over a range of mean eruption rates for both conditions, but is Ψ dependent for decreasing eruption rates. Significant resurfacing ($\geq$20% of flow resurfaced), however, is most likely to occur at low mean eruption rates and low Ψ for decreasing (condition 1) and increasing (condition 2) eruption rates.
5. Breakouts at the flow margin are widespread and can activate the entire flow front when eruption rate increases, flow rate is high, and crust is weak (high Ψ). Breakouts at the flow margins occur at discrete locations when flow rate is low, crust is strong (low Ψ), and the duration in change in eruption rate is long (for decreasing eruption rates) or short (for increasing eruption rates).
6. Inflation occurs when an extensive, coherent crust is present. While favored at low and intermediate eruption rates, inflation can occur or survive an abrupt increase in eruption rate when a strong crust is present, usually associated with condition 2 at low to intermediate Ψ.
7. Tubes were more difficult to simulate in the laboratory than other emplacement modes. Tubes required the formation of a stable crust that allowed flow beneath it. The inability to reproduce tubes may either lie in the intended unsteadiness of the experiment or the duration of the experiments. The unsteadiness appears to disrupt tube formation whereas the short duration of the experiments may not allow sufficient time for tubes to develop.
8. The duration of eruption is an important control on establishment of a coherent, insulating crust and the likelihood and extent of emplacement modes occurring. Short variations in the eruption rate, specifically for decreasing flow rates, may not extrude enough material to trigger the expansion of the flow field. Long variations in eruption rate, however, can have large impacts on flow dimension and the significance of emplacement modes.
9. Observations from the early stages of the Fagradalsfjall eruption support that decreasing effusion rates lead to crust-strengthening dependent modes of emplacement (such as tubes) whereas increasing effusion rates lead to crust-disrupting modes, such as resurfacing and marginal breakouts.

Funding

This research did not receive any specific grant from funding agencies in the public, commercial, or not-for-profit sectors.

Data availability

The data presented here, which includes experimental runs, figures, and photographs of the wax flows, are available via the ASU Library's Research Data Repository (https://doi.org/10.48349/ASU/LTWBGY).

Author statement

Sean Peters: Conceptualization, methodology, investigation, data

curation, formal analysis, investigation, writing – original draft preparation, writing - reviewing, and editing; Amanda Clarke: Supervision, conceptualization, methodology, investigation, writing – original draft preparation, writing - reviewing, and editing; Erika Rader: writing – reviewing and editing.

Declaration of Competing Interest

The authors declare that they have no known competing financial interests or personal relationships that could have appeared to influence the work reported in this paper.

Data availability

The data presented here, which includes experimental runs, figures, and photographs of the wax flows, are available via the ASU Library's Research Data Repository (https://doi.org/10.48349/ASU/LTWBGY)

Acknowledgements

Special thanks to Christopher P. Mount for assisting with laboratory setup and experimental runs. Additionally, we would like to thank Rebecca DeGraffenried and an anonymous reviewer for thorough discussions which have greatly improved the quality of this manuscript.

References

Abramoff, M.D., Magalhaes, P.J., Ram, S.J., 2004. Image processing with image. J. Biophoton. Int. 11, 36–42.
Bailey, J.E., Harris, A.J.L., Dehn, J., Calvari, S., Rowland, S.K., 2006. The changing morphology of an open channel on Mt. Etna. Bull. Volcanol. 68, 497–515. https://doi.org/10.1007/s00445-005-0025-6.
Baloga, S., Pieri, D., 1986. Time-dependent profiles of lava flows. J. Geophys. Res. 91 (B9), 9543–9552.
Belousov, A., Belousov, M., Edwards, B., Volynets, A., Melnikov, D., 2015. Overview of the precursors and dynamics of the 2012–13 basaltic fissure eruption of Tolbachik Volcano, Kamchatka, Russia. J. Volcanol. Geotherm. Res. 307, 22–37. https://doi.org/10.1016/j.jvolgeores.2015.04.009.
Blake, S., Bruno, B.C., 2000. Modelling the emplacement of compound lava flows. Earth Planet. Sci. Lett. 184, 181–197.
Bonny, E., Wright, R., 2017. Predicting the end of lava flow-forming eruptions from space. Bull. Volcanol. 79, 52. https://doi.org/10.1007/s00445-017-1134-8.
Brown, D., 2009. Video modeling with tracker. In: AAPT Topical Conference: Computer Modeling in the Introductory Course. AAPT Summer Meeting.
Calvari, S., Neri, M., Pinkerton, H., 2002. Effusion rate estimations during the 1999 summit eruption on Mount Etna, and growth of two distinct lava flow fields. J. Volcanol. Geotherm. Res. 119, 107–123.
Capello, A., Herault, A., Bilotta, G., Ganci, G., Del Negro, C., 2015. MAGFLOW: a physics-based model for the dynamics of lava flow emplacement. Geol. Soc. Lond. Spec. Publ. 426, 357–373. https://doi.org/10.1144/SP426.16.
Carr, B.B., Clarke, A.B., Vanderkluysen, L., Arrowsmith, J.R., 2019. Mechanisms of lava flow emplacement during an effusive eruption of Sinabung Volcano (Sumatra, Indonesia). J. Volcanol. Geotherm. Res. 382, 137–148. https://doi.org/10.1016/j.jvolgeores.2018.03.002.
Cashman, K.V., Kerr, R.C., Griffiths, R.W., 2006. A laboratory model of surface crust formation and disruption on lava flows through non-uniform channels. Bull. Volcanol. 68, 753–770. https://doi.org/10.1007/s00445-005-0048-z.
Connor, L.J., Connor, C.B., Meliksetian, K., Savov, I., 2012. Probabilistic approach to modelling lava flow inundation: a lava flow hazard assessment for a nuclear facility in Armenia. J. Appl. Volcan. 1, 3.
Crisp, J.A., 1984. Rates of Magma emplacement and volcanic output. J. Volcanol. Geotherm. Res. 20, 177–221.
Danes, Z.F., 1972. Dynamics of lava flows. J. Geophys. Res. 77 (8), 1430–1432.
DeGraffenried, R., Hammer, J., Dietterich, H., Perroy, R., Patrick, M., Shea, T., 2021. Evaluating lava flow propagation models with a case study from the 2018 eruption of Kīlauea Volcano, Hawai'I. Bull. Volcanol. 83 (11), 1–19.
Del Negro, C., Capello, A., Neri, M., Bilotta, G., Herault, A., Ganci, G., 2013. Lava flow hazards at Mt. Etna: constraints impose by eruptive history and numerical simulations. Sci. Rep. 3, 3493. https://doi.org/10.1038/srep03493.
Dietterich, H.R., Lev, E., Chen, J., Richardson, J.A., Cashman, K.V., 2017. Benchmarking computational fluid dynamics models of lava flow simulation for hazard assessment, forecasting, and risk management. J. Appl. Volcano 6, 9. https://doi.org/10.1186/s13617-017-0061-x.
D'Michieli Vitturi, M., Tarquini, S., 2018. Mr Lava Loba: a new probabilistic model for the simulation of lava flows as a settling process. J. Volcanol. Geotherm. Res. 349, 323–334.
Dragoni, M., Tallarico, A., 1994. The effect of crystallization on the rheology and dynamics of lava flows. J. Volcanol. Geotherm. Res. 59, 241–252.
Favalli, M., Pareschi, M.T., Neri, A., Isola, I., 2005. Forecasting lava flow paths by a stochastic approach. Geophys. Res. Lett. 32, L03305. https://doi.org/10.1029/2004GL021718.
Felpeto, A., Arana, V., Ortiz, R., Astiz, M., Garcia, A., 2001. Assessment and modelling of lava flow hazard on Lanzarote (Canary Islands). Nat. Hazards 23, 247–257.
Fink, J.H., Fletcher, R.C., 1978. Ropy pāhoehoe: surface folding of a viscous fluid. J. Volcanol. Geotherm. Res. 4, 151–170.
Fink, J.H., Griffiths, R.W., 1990. Radial spreading of viscous-gravity currents with solidifying crust. J. Fluid Mech. 221, 485–509.
Fink, J.H., Griffiths, R.W., 1992. A laboratory analog study of the surface morphology of lava flows extruded from point and line sources. J. Volcanol. Geotherm. Res. 54 (1–2) https://doi.org/10.1016/0377-0273(92)90112-Q.
Fink, J.H., Park, S.O., Greeley, R., 1983. Cooling and deformation of sulfur flows. Icarus 56, 38–50.
Francis, P., Oppenheimer, C., 2003. Volcanoes, 2nd edition. Oxford Univ. Press.
Ganci, G., Vicari, A., Cappello, A., Nero, C.D., 2012. An emergent strategy for volcano hazard assessment: from thermal satellite monitoring to lava flow modelling. Remote Sens. Environ. 119, 197–207. https://doi.org/10.1016/j.rse.2011.12.021.
Garry, W.B., Gregg, T.K.P., Soule, S.A., Fornari, D.J., 2006. Formation of submarine lava channel textures: insights from laboratory simulations. J. Geophys. Res. 111, B03104. https://doi.org/10.1029/2005JB003796.
Greeley, R., 1972. Additional observations of actively forming lava tubes and associated structures, Hawaii. Modern Geol. 3, 157–160.
Greeley, R., 1987. The role of lava tubes in Hawaiian volcanoes. In: Volcanism in Hawaii, USGS Proff. Paper, pp. 1589–1602 chapter 59.
Greeley, R., Spudis, P.D., 1981. Volcanism on Mars. Rev. Geophys. 19 (1), 13–41. https://doi.org/10.1029/RG019i001p00013.
Gregg, T.K.P., Fink, J.H., 1996. Quantification of extraterrestrial lava flow effusion rates through laboratory simulations. J. Geophys. Res. 101 (E7), 16891–16900, 96JE01254.
Gregg, T.K.P., Fink, J.H., 2000. A laboratory investigation into the effects of slope on lava flow morphology. J. Volcanol. Geotherm. Res. 96, 145–159.
Gregg, T.K.P., Keszthelyi, L.P., 2004. The emplacement of pāhoehoe toes: field observations and comparison to laboratory simulations. Bull. Volcanol. 66, 381–391. https://doi.org/10.1007/s00445-003-0319-5.
Gregg, T.K.P., Smith, D.K., 2003. Volcanic investigations of the Puna Ridge, Hawai'i: relations of lava flow morphologies and underlying slopes. J. Volcanol. Geotherm. Res. 126, 63–77.
Griffiths, R.W., 2000. The dynamics of lava flows. Annu. Rev. Fluid Mech. 32, 477–518.
Griffiths, R.W., Fink, J.H., 1992. The morphology of lava flows in planetary environments: predictions from analog experiments. J. Geophys. Res. Solid Earth 97 (B13), 19739–19748.
Griffiths, R.W., Fink, J.H., 1993. Effects of surface cooling on the spreading of lava flows and domes. J. Fluid Mech. 252, 667–702.
Griffiths, R.W., Fink, J.H., 1997. Solidifying Bingham extrusions: a model for the growth of silicic lava domes. J. Fluid Mech. 347, 13–36.
Hallsworth, M.A., Huppert, H.E., Sparks, R.S.J., 1987. A laboratory simulation of basaltic lava flows. Mod. Geol. 11, 93–107.
Harris, A.J.L., Rowland, S.K., 2001. FLOWGO: a kinematic thermo-rheological model for lava flowing in a channel. Bull. Volcanol. 63, 20–44. https://doi.org/10.1007/s004450000120.
Hidaka, M., Goto, A., Umino, S., Fujita, E., 2005. VTFS project: Development of the lava flow simulation code LavaSIM with a model for three-dimensional convection, spreading, and solidification. Geochem. Geophys. Geosyst. 6 (7) https://doi.org/10.1029/2004GC000869.
Hoblitt, R.P., Orr, T.R., Heliker, C., Denlinger, R.P., Hon, K., Cervelli, P.F., 2012. Inflation rates, rifts, and bands in a pāhoehoe sheet flow. Geosphere 8 (1), 179–195. https://doi.org/10.1130/GES00656.1.
Hon, K., Kauahikaua, J., Denliger, R., Mackay, K., 1994. Emplacement and inflation of pāhoehoe sheet flows: observations and measurements of active lava flows of Kilauea volcano, Hawaii. Geol. Soc. Am. Bull. 106, 351–370.
Hulme, G., 1974. The Interpretation of Lava Flow Morphology. Geophys. J. Int. 39 (2), 361–383. https://doi.org/10.1111/j.1365-246X.1974.tb05460.x.
Ivanov, M.A., Head, J.W., 2013. The history of volcanism on Venus. Planet. Space Sci. 84, 66–92.
Jasak, H., Jemcov, A., Tukivić, Z., 2007. OpenFOAM: a C++ library for complex physics simulations. In: Intern. Workshop on Coupled Method. in Numerical Dynamics. IUC, pp. 1–20.
Kerr, R.C., Griffiths, R.W., Cashman, K.V., 2006. Formation of channelized lava flows on an unconfined slope. J. Geophys. Res. 111, B10206. https://doi.org/10.1029/2005JB004225.
Lev, E., Rumpf, E., Diettrich, H., 2019. Analog experiments of lava flow emplacement. Ann. Geophys. 62 (2) https://doi.org/10.4401/ag-7843.
Malin, M.C., 1980. Lengths of Hawaiian lava flows. Geology 8, 306–308.
Patrick, M.R., Dietterich, H.R., Lyons, J.J., Diefenbach, A.K., Parcheta, C., Anderson, K. R., Namiki, A., Sumita, I., Shiro, B., Kauahikaua, J.P., 2019. Cyclic lava effusion during the 2018 eruption of Kīlauea Volcano. Science 366 (6470). https://doi.org/10.1126/science.aay9070.
Peters, S.I., Christensen, P.R., Clarke, A.B., 2021. Lava flow eruption conditions in the Tharsis Volcanic Province on Mars. J. Geophys. Res. Planets 126. https://doi.org/10.1029/2020JE006791.
Peterson, D.W., Tilling, R.I., 1980. Transition of basaltic lava from pāhoehoe to aa, Kilauea volcano, Hawaii: field observations and key factors. J. Volcanol. Geotherm. Res. 7, 271–293.
Pinkerton, H., 1987. Factors affecting the morphology of lava flows. Endeav. New Ser. 11 (2), 73–79.

Rader, E., Vanderkluysen, L., Clarke, A., 2017. The role of unsteady effusion rates on inflation in long-lived lava flow fields. Earth Planet. Sci. Lett. 477, 73–83.
Rowland, S.K., Harris, A.J.L., Garbeil, H., 2004. Effects of Martian conditions on numerically modeled, cooling-limited, channelized lava flows. J. Geophys. Res. 109, E10010. https://doi.org/10.1029/2004JE002288.
Self, S., Thordarson, T., Kesthelyi, L., Walker, G.P.L., Hon, K., Murphy, M.T., Long, P., Finnemore, S., 1996. A new model for the emplacement of Colombia River basalts as large, inflated pāhoehoe lava flow fields. Geophys. Res. Lett. 23 (19), 2689–2692.
Sheth, H.C., 2006. Large Igneous Provinces (LIPs): definition, recommended terminology, and a hierarchical classification. Earth Sci. Rev. 85, 117–124.
Soule, S.A., Cashman, K.V., 2004. The mechanical properties of solidified polyethylene glycol 600, an analog for lava crust. J. Volcanol. Geotherm. Res. 129, 139–153.
Tarquini, S., d'Michieli Vitturi, M., 2014. Influence of fluctuating supply on the emplacement dynamics of channelized lava flows. Bull. Volcanol. 76, 801. https://doi.org/10.1007/s00445-014-0801-2.
Tuffen, H., James, M.R., Castro, J.M., Schipper, C.I., 2013. Exceptional mobility of an advancing rhyolitic obsidian flow at Cordon Caulle volcano in Chile. Nat. Commun. 4, 2709. https://doi.org/10.1038/ncomms3709.
Vicari, A., Alexis, H., Del Negro, C., Coltelli, M., Marsella, M., Proietti, C., 2007. Modelling of the 2001 lava flow at Etna volcano by cellular automata approach. Environ. Model. Softw. 22, 1465–1471.
Wadge, G., 1981. The variation of magma discharge during basaltic eruptions. J. Volcanol. Geotherm. Res. 11, 139–168.
Walker, G.P.L., 1973. Lengths of lava flows. Phil. Trans. R. Soc. Lond. A 274, 107–118.